

**EUROPEAN ORGANISATION FOR NUCLEAR RESEARCH
CERN – A&B DEPARTMENT**

AB-Note-2006-033 ABP

END-TO-END SIMULATIONS OF LINAC4

S. Lanzone, J.B. Lallement, A. Lombardi, E. Sargsyan

Abstract

Linac4 is a new H⁺ linear accelerator presently studied at CERN. This machine consists of normal-conducting structures operating at 352.2 MHz and 704.4 MHz re-using the RF equipment from the decommissioned LEP collider. It consists of a 95 keV H⁺ source, a 352 MHz RFQ bringing the energy the energy to 3 MeV, a Chopper line, a 352 MHz Drift Tube Linac bringing the energy to 40 MeV, a 352 MHz Coupled Cavity Drift Tube Linac bringing the energy to 90 MeV and a 704 MHz Side Coupled Linac bringing the energy to 160 MeV. Each section is designed and optimized as stand-alone machines for a good transmission and minimum possible emittance growth. End-to-end simulations starting from the RFQ have been carried out in order to validate and compare the multiparticle simulation codes PATH Manager and TRACEWIN used for beam dynamics calculations as well as to perform a global optimization of the structures in the context of a complex machine.

Geneva, Switzerland
May 2006

Contents

Introduction	3
1. Beam dynamics in the Chopper Line	4
1.1 Beam from the RFQ, unmatched case ($I = 0$ mA).....	4
1.2 Beam from the RFQ, matched case ($I = 69.9$ mA).....	7
1.3 Summary of Section 1.....	11
2. Beam dynamics in the DTL	11
2.1 Test beam, $I = 0$ mA.....	11
2.2 Test beam, $I = 65$ mA.....	15
2.3 Beam from Chopper Line, unmatched case ($I = 0$ mA).....	18
2.4 Beam from Chopper Line, matched case.....	21
2.5 Summary of Section 2.....	23
3. Beam dynamics in the CCDTL	23
3.1 Test beam, $I = 0$ mA.....	23
3.2 Test beam, $I = 65$ mA.....	26
3.3 Beam from the DTL, unmatched case ($I = 0$ mA).....	29
3.4 Beam from the DTL, matched case.....	31
3.5 Summary for the CCDTL.....	34
4. Beam dynamics in the SCL	34
4.1 Test beam, $I = 0$ mA.....	35
4.2 Test beam, $I = 130$ mA.....	38
4.3 Beam from the CCDTL, unmatched case ($I = 0$ mA).....	40
4.4 Beam from the CCDTL, matched case.....	44
4.5 Summary for the SCL.....	48
Conclusion and outlook	48
Reference	48

Introduction

Linac4 is a new H⁻ linear accelerator presently studied at CERN. This machine consists of normal-conducting structures operating at 352.2 MHz and 704.4 MHz (Fig. 1) re-using the RF equipment from the decommissioned LEP collider. It is designed to replace the existing Linac2 and to inject the beam into the CERN PS Booster (PSB) at 160 MeV instead of present 50 MeV injection energy to overcome the space-charge limitation. At the same time it is a front-end for the future high power 3.5 GeV superconducting linac (SPL) [1].

The layout of LINAC4 is sketched in Fig 1. It consists of a RF volume source (identical to the one in DESY) which provides an H⁻ beam at 35 kV further post-accelerated to 95keV. The first RF acceleration (from 95keV to 3 MeV) is done by a Radio Frequency Quadrupole (the IPHI RFQ from CEA [2]). The RFQ resonates at 352 MHz, is 6 m long and it is powered by a 1 MW Klystron. At 3 MeV the beam enters a 3.6 meter long chopper line, consisting of 11 quadrupoles, 3 bunchers and two sets of deflecting plates. This system has the capability of removing micro-bunches on the RF scale and rematch the beam to the subsequent system of accelerators. A rudimentary collimation is also performed in this line. The beam is then further accelerated to 40 MeV in a conventional Drift Tube Linac at 352 MHz. The DTL, subdivided in 3 tanks, is 13.4 meters long and it is powered by 5 klystrons for a total power of 4 MW. Each of the 82 drift tubes is equipped with a Permanent Magnet Quadrupole. At 40 MeV the velocity of the beam is such as to allow the transition to structures which don't follow cell-by-cell the beam velocity profile. In LINAC4 the acceleration from 40 to 90 MeV is provided by a Cell-Coupled Drift Tube Linac at 352 MHz. The CCDTL is made of 24 tanks of 3 cells each for a total length of 25.3 meters. Four tanks are powered by the same klystron, for a total of 8 klystrons delivering 6.5 MW. The focusing is provided by electromagnetic quadrupoles placed outside each tank. The acceleration from 90 to 160 MeV is done in a Side Coupled Linac resonating at 704 MHz. The SCL is made of 20 tanks of 11 cells each for a total of 28 m, powered by 4 klystrons delivering 12 MW. Focusing is provided by 20 Electromagnetic Quadrupoles.

This brings the total length of the linac to 80 m, for a total of 18 klystrons. The duty cycle of LINAC4 is 0.1% when used as injector to the PS booster but it grows to 3-4% if we consider its potential use as front-end of a high power proton driver like the SPL [1]. During the design phase we have decided to take as effective duty cycle the value of 15%: this value is used through the paper unless otherwise indicated.

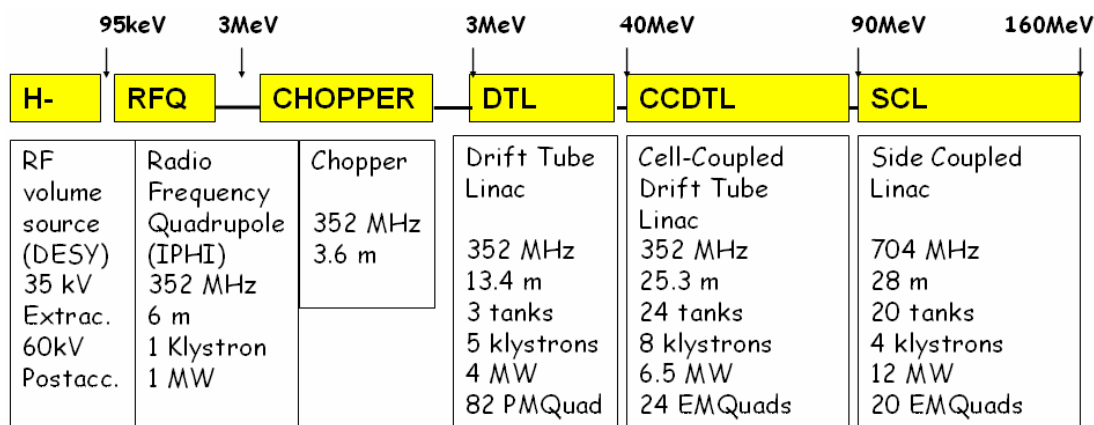


Figure 1: Layout of the Linac4

The Chopper Line and following accelerating structures are designed and optimized as stand-alone machines for a good transmission (beam losses <1W/m) and minimum possible emittance growth. The purpose of the work presented in this note is to validate/compare the multiparticle simulation codes PATH Manager and TRACEWIN used for beam dynamics calculations as well as to perform a global optimization of the structures in the context of a complex machine. Therefore end-to-end simulations of the Linac4 have been carried out. At this point we lack for simulation data of the H⁻ ion source and the simulations start with a generated uniform beam distribution at the input of the IPHI RFQ [2], designed by CEA and IN2P3. Beam dynamics simulations in the RFQ are performed using Toutatis code and the RFQ is under construction, thus the actual code comparison and optimization of the structures starts from the Chopper Line.

End-to-end simulation of Linac4 with PATH and TRACEWIN

The end-to-end simulation set-up comprises of the IPHI RFQ, the Chopper Line, the DTL, the CCDTL and the SCL. The beam dynamics in each structure except the RFQ has been studied and analyzed separately using as an input beam the output from the previous structure. Simulations are carried out first for zero current to check and compare the structures in two codes in the absence of space-charge effects and then with nominal current. For the simulations with current a 2D space-charge routine has been used in both codes, which gives more pessimistic results for transverse emittance growth with respect to the 3D space-charge routine.

1. Beam dynamics in the Chopper Line

The Chopper Line operates at 352.2 MHz and the input beam energy is 3 MeV with a bunch current of 69.9 mA per RF period. The number of particles is 49940. Twiss parameters of the Chopper input beam are reported in Table 1.

Table 1: Input beam parameters of the Chopper Line

	α	β	$\epsilon_{RMS,N}$	$\epsilon_{90\%,N}$
x	0.96	0.20 mm/ π mrad	0.27 π mm mrad	1.14 π mm mrad
y	-1.66	0.43 mm/ π mrad	0.27 π mm mrad	1.13 π mm mrad
long	0.26	594.71 deg/ π MeV	0.14 π deg MeV	0.64 π deg MeV

The beam comes from the RFQ output. The Chopper Line structure is 3.698 m. The simulations are carried out using both PATH and TRACEWIN codes.

1.1 Beam from the RFQ, unmatched case ($I = 0$ mA)

In order to check the structure, the space-charge effects are disabled in the first simulation by running the structure with 0 mA current. In Figure 2 the RMS beam size sizes along the Chopper Line obtained in PATH and TRACEWIN are compared. Figure 3 compares the RMS normalized emittances along the structure.

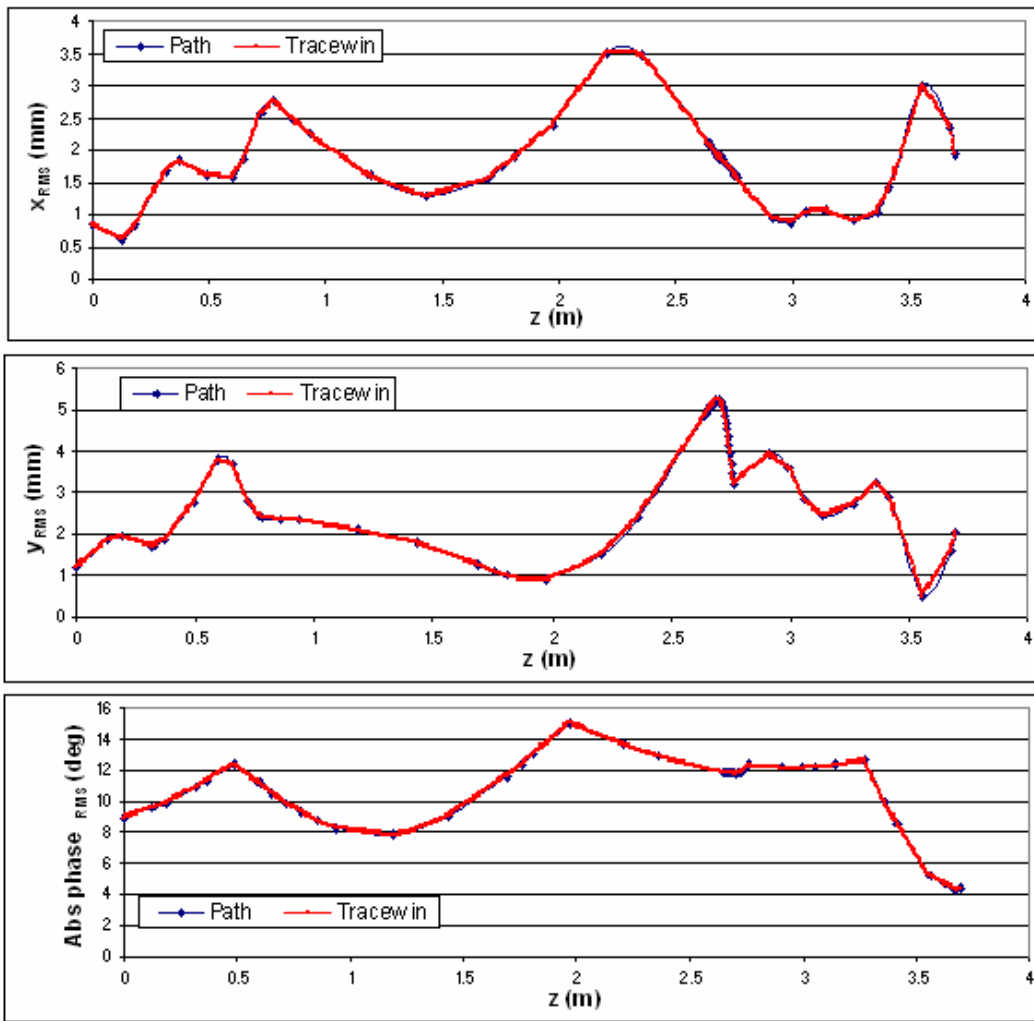


Figure 2: RMS beam size along the Chopper Line

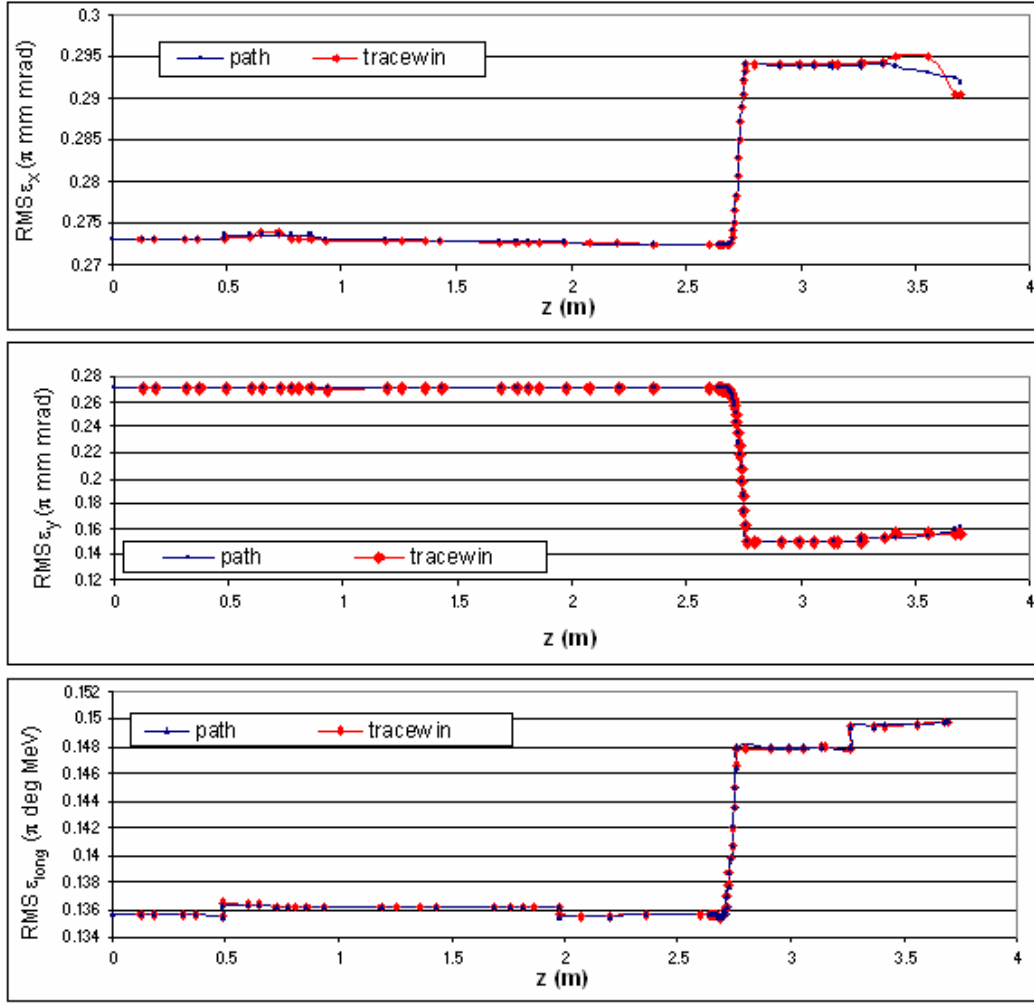


Figure 3: RMS normalized emittance envelopes along the Chopper Line

The transmission is 63.88% in PATH and 63.86% in TRACEWIN and about 36% of the particles are lost in the dump.

The Twiss parameters of the beam at the end of the Chopper Line obtained with PATH and TRACEWIN are summarized in Table 2 and 3 respectively. The beam phase space plots are presented in Figure 4 and 5.

Table 2: Chopper Line output beam parameters in PATH

	α	β	$\epsilon_{RMS,N}$	$\epsilon_{90\%,N}$
x	11.27	1.03 mm/ π mrad	0.29 π mm mrad	1.18 π mm mrad
y	-22.57	2.07 mm/ π mrad	0.16 π mm mrad	0.65 π mm mrad
z	0.29	132.37 deg/ π MeV	0.15 π deg MeV	0.67 π deg MeV

Table 3: Chopper Line output beam parameters in TRACEWIN

	α	β	$\epsilon_{RMS,N}$	$\epsilon_{90\%,N}$
x	11.31	1.03 mm/ π mrad	0.29 π mm mrad	1.18 π mm mrad
y	-23.38	2.15 mm/ π mrad	0.16 π mm mrad	0.62 π mm mrad
z	0.30	132.72 deg/ π MeV	0.15 π deg MeV	0.68 π deg MeV

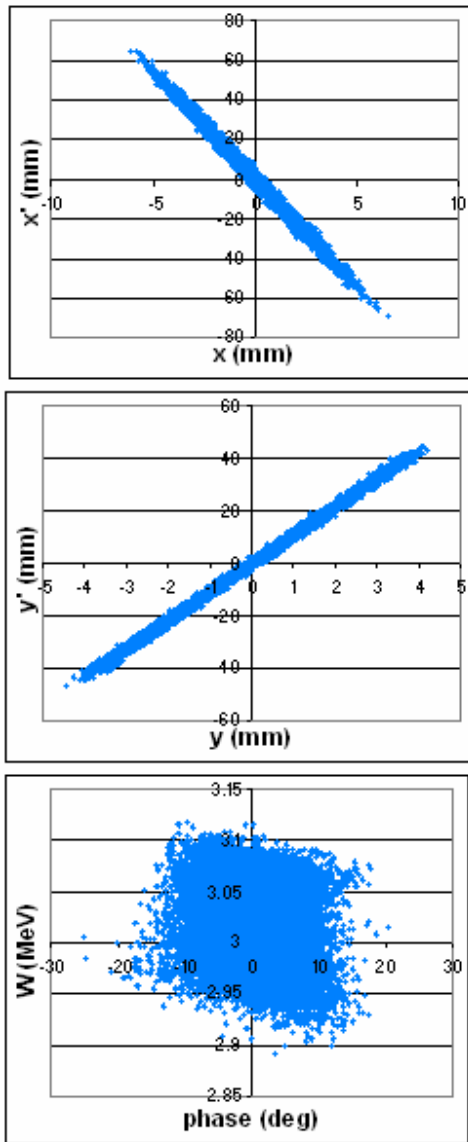


Figure 4: Beam phase space in PATH

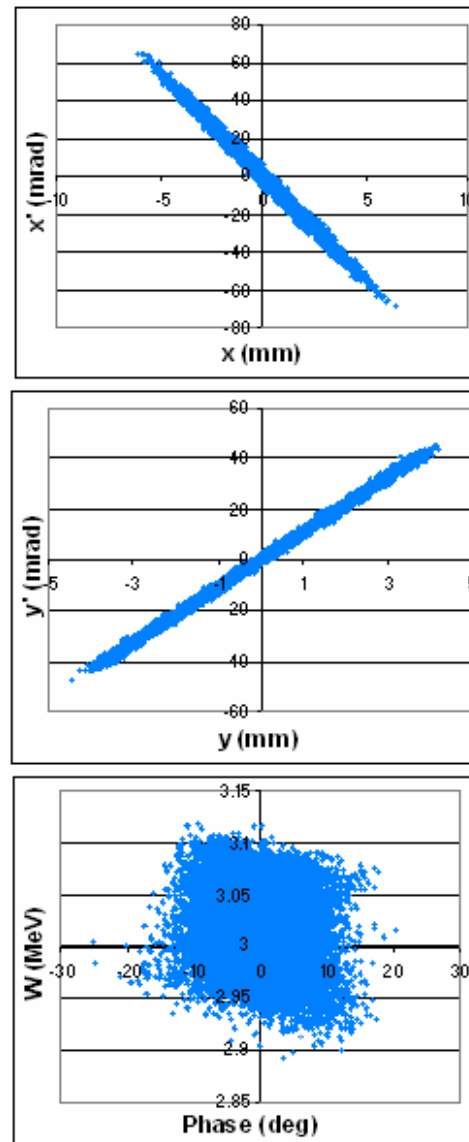


Figure 5: beam phase space in TRACEWIN

1.2 Beam from the RFQ, matched case ($I = 69.9$ mA)

Beam parameters have been compared with space-charge effects for the current of 69.9 mA using a 2D space charge routine (Rings of Charge in PATH and Picnir in TRACEWIN) in both codes.

The RMS beam size sizes along the Chopper Line obtained in PATH and TRACEWIN are compared in Figure 6.

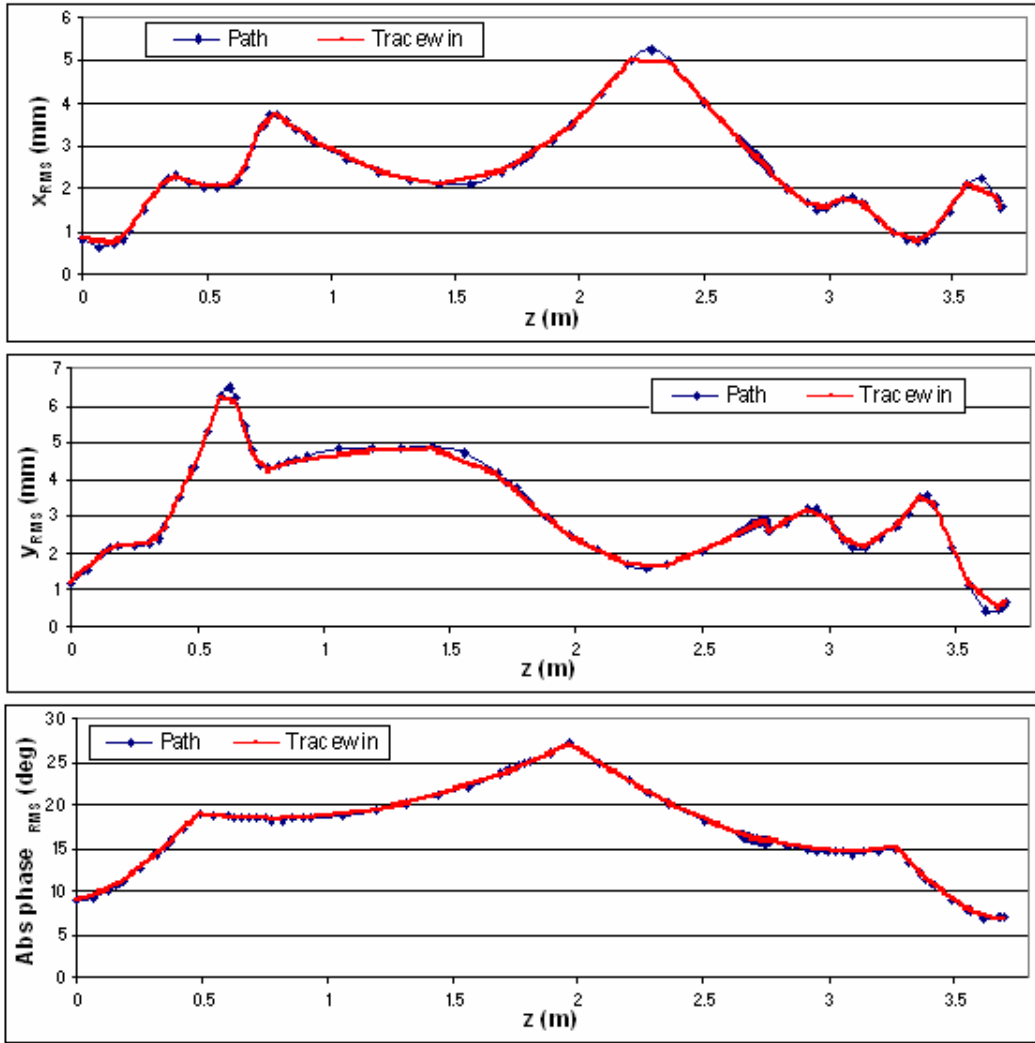


Figure 6: RMS beam size along the Chopper Line

The RMS and 90% emittance growth in the Chopper Line are reported in the Table 4 and Table 5 respectively.

Table 4: RMS emittance growth in the Chopper Line

	ϵ_x	ϵ_y	ϵ_{long}
PATH	23.9%	7.6%	18.6%
TRACEWIN	21.0%	3.5%	17.5%

Table 5: 90% emittance growth in the Chopper Line

	ϵ_x	ϵ_y	ϵ_{long}
PATH	26.2%	17.5%	16.5%
TRACEWIN	21.9%	10.8%	15.3%

The RMS normalized emittances along the Chopper Line are compared in Figure 7 for both codes. The maximum difference between the emittance values in two codes is $\Delta\epsilon/\epsilon = 3-4\%$ (for ϵ_y).

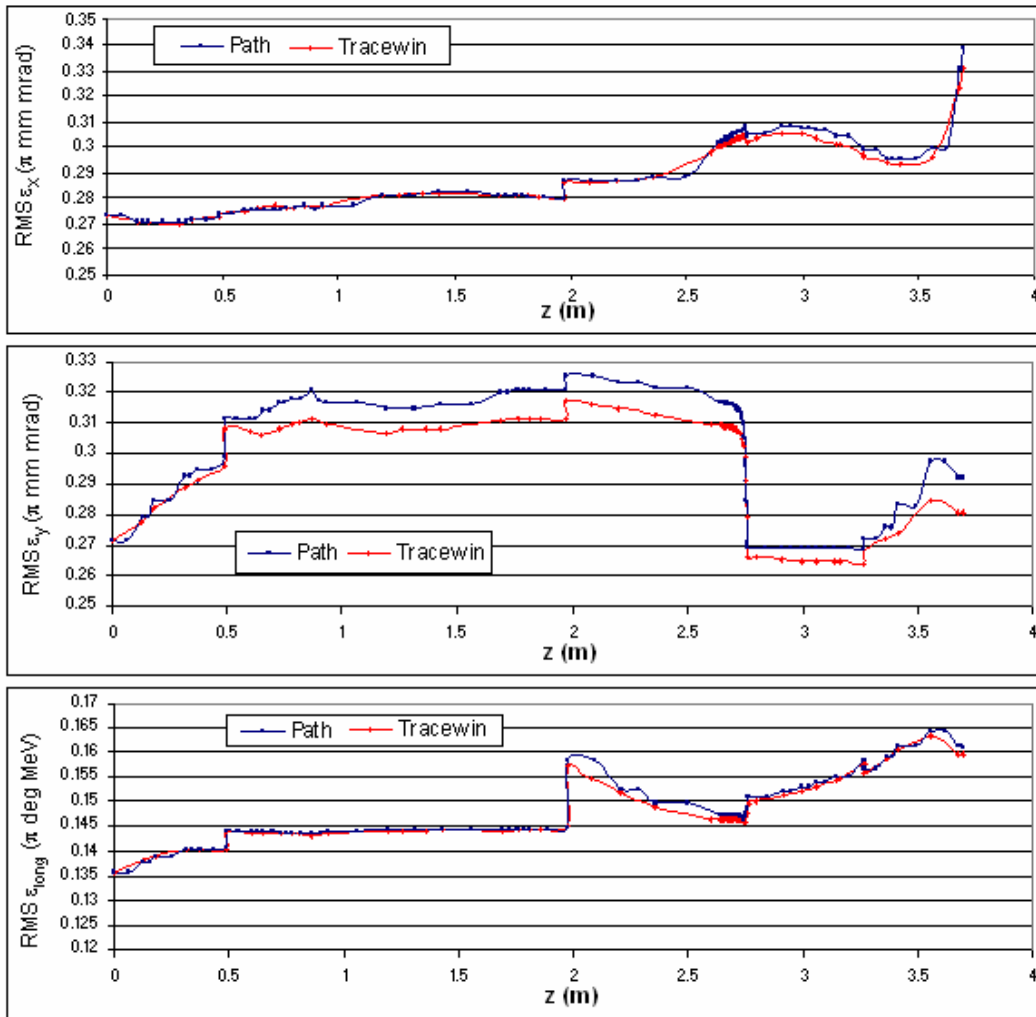


Figure 7: RMS normalized emittances along the Chopper Line

The transmission in the line is 88.52% in PATH and 88.95% in TRACEWIN, so the output current is 61.9 mA and 62.2 mA respectively. The losses are shown in Figure 8: about 63% of the lost particles are concentrated in the final part of the dump.

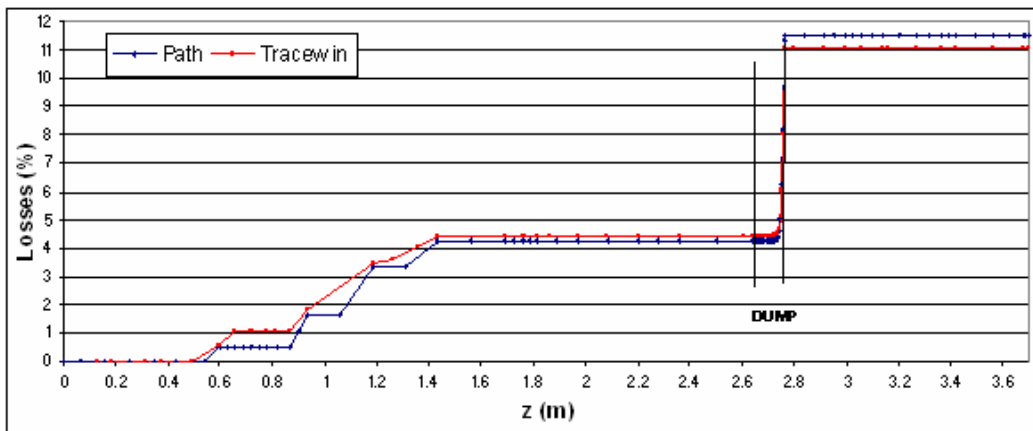


Figure 8: Losses along the Chopper Line

Twiss parameters of the beam at the end of the Chopper Line obtained with PATH and TRACEWIN are summarized in Table 6 and Table 7 respectively. Beam phase space plots are presented in Figure 9 and 10.

Table 6: Chopper Line output beam parameters in PATH

	α	β	$\epsilon_{RMS,N}$	$\epsilon_{90\%,N}$
x	4.66	0.59 mm/ π mrad	0.34 π mm mrad	1.43 π mm mrad
y	-1.62	0.13 mm/ π mrad	0.29 π mm mrad	1.32 π mm mrad
z	0.28	307.94 deg/ π MeV	0.16 π deg MeV	0.73 π deg MeV

Table 7: Chopper Line output beam parameters in TRACEWIN

	α	β	$\epsilon_{RMS,N}$	$\epsilon_{90\%,N}$
x	4.70	0.60 mm/ π mrad	0.33 π mm mrad	1.39 π mm mrad
y	-1.72	0.13 mm/ π mrad	0.28 π mm mrad	1.26 π mm mrad
z	0.30	291.29 deg/ π MeV	0.16 π deg MeV	0.73 π deg MeV

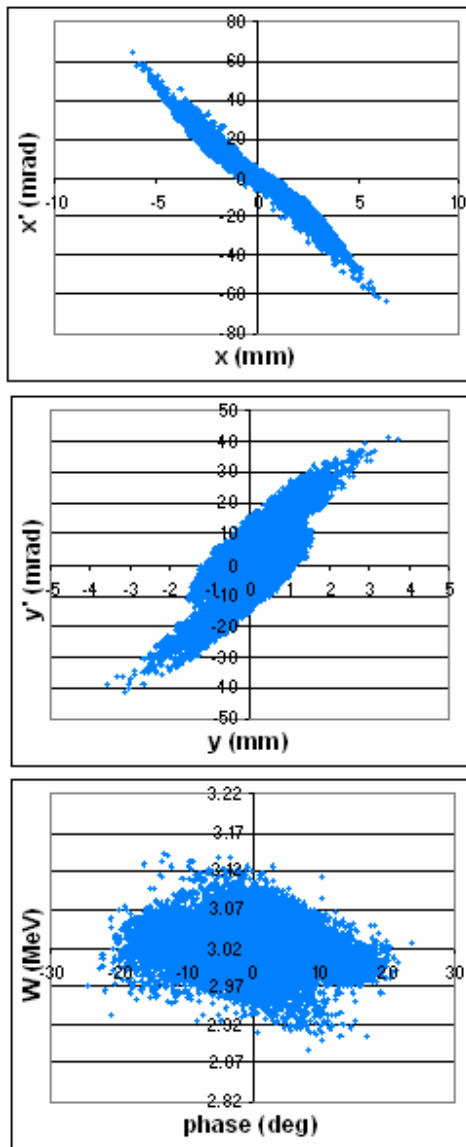


Figure 9: Beam phase space in PATH

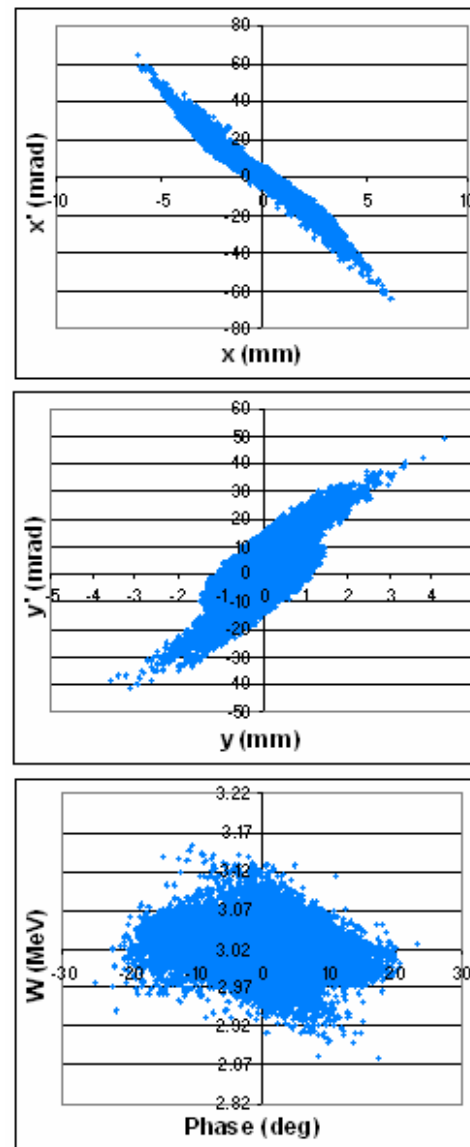


Figure 10: Beam phase space in TRACEWIN

1.3 Summary of Section 1

The results of comparison between the two codes are quite good both with and without space-charge effect. The beam characteristics obtained with both codes are similar. With space-charge effects the PATH output beam is a little more spread compared to the TRACEWIN one; the maximum difference between Twiss parameters is about $\Delta\alpha/\alpha \sim 9\%$ and $\Delta\beta/\beta \sim 5\%$. For this case the difference between both the RMS emittances and the losses is big, so the difference in emittances can probably be due to the difference in losses.

2. Beam dynamics in the DTL

As in the previous section, in order to check the structure the first simulation has been done without space-charge effects and with a test beam generated at the input of the DTL. Further, the beam coming from the Chopper Line has been used for simulations with and without space-charge.

2.1 Test beam, $I = 0$ mA

The generated input beam characteristics are:

- Number of particles = 50000
- $f = 352.2$ MHz
- $E_{in} = 3.01924$ MeV
- Twiss parameters:

	α	β	$\epsilon_{RMS,N}$
x	4.7	0.6 mm/ π mrad	0.28 π mm mrad
y	-1.7	0.13 mm/ π mrad	0.28 π mm mrad
long	-0.3	291.23 deg/ π MeV	0.17 π deg MeV

For 0 mA current the transmission is 100% in both codes. The energy evolution is plotted in Figure 11. The output beam energy is 39.89 MeV in PATH and 39.84 MeV in TRACEWIN.

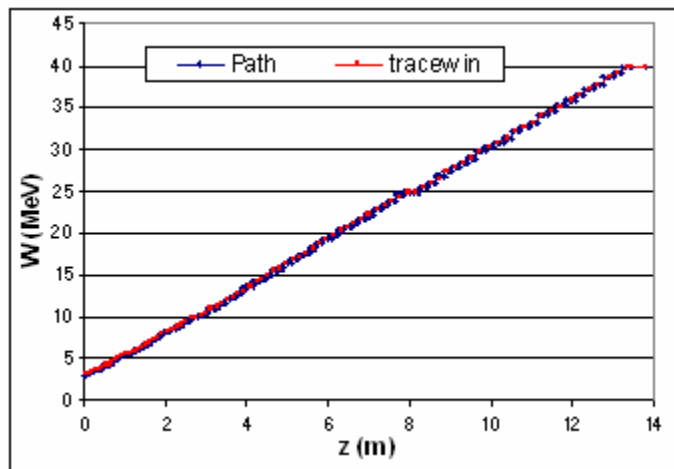


Figure 11: Energy evolution along the DTL, test beam, $I = 0$ mA

The DTL output beam phase space plots are presented in Figure 12 and Figure 13 and Twiss parameters are reported in Table 8 and Table 9. RMS beam size envelopes and emittances are plotted in Figures 14 and 15.

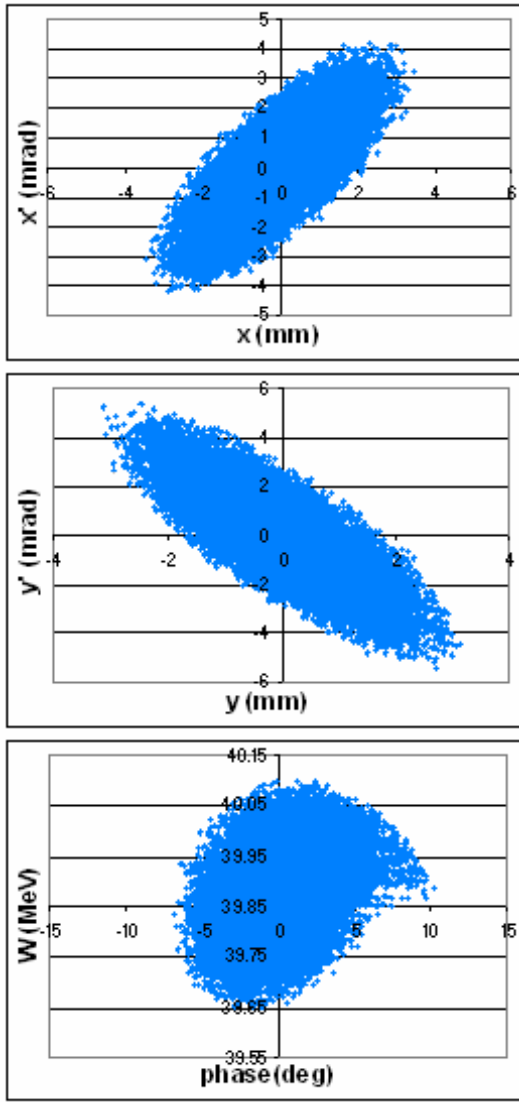


Figure 12: DTL output beam in PATH,
test beam, $I = 0$ mA

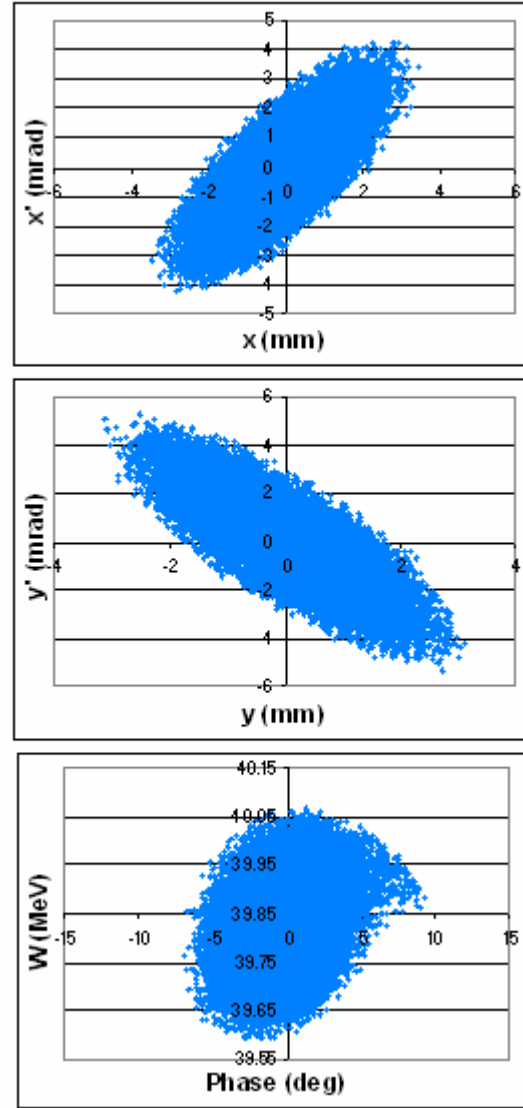


Figure 13: DTL output beam in TRACEWIN,
test beam, $I = 0$ mA

Table 8: Twiss parameters of the DTL output beam in TRACEWIN, test beam, $I = 0$ mA

	α	β	$\epsilon_{RMS,N}$	$\epsilon_{90\%,N}$
x	-1.16	1.17 mm/ π mrad	0.28 π mm mrad	1.28 π mm mrad
y	1.28	0.97 mm/ π mrad	0.28 π mm mrad	1.28 π mm mrad
long	-0.28	26.41 deg/ π MeV	0.17 π deg MeV	0.78 π deg MeV

Table 9: Twiss parameters of the DTL output beam in PATH, test beam, $I = 0$ mA

	α	β	$\epsilon_{RMS,N}$	$\epsilon_{90\%,N}$
x	-1.13	1.17 mm/ π mrad	0.28 π mm mrad	1.27 π mm mrad
y	1.32	0.98 mm/ π mrad	0.28 π mm mrad	1.28 π mm mrad
long	-0.31	30.21 deg/ π MeV	0.17 π deg MeV	0.77 π deg MeV

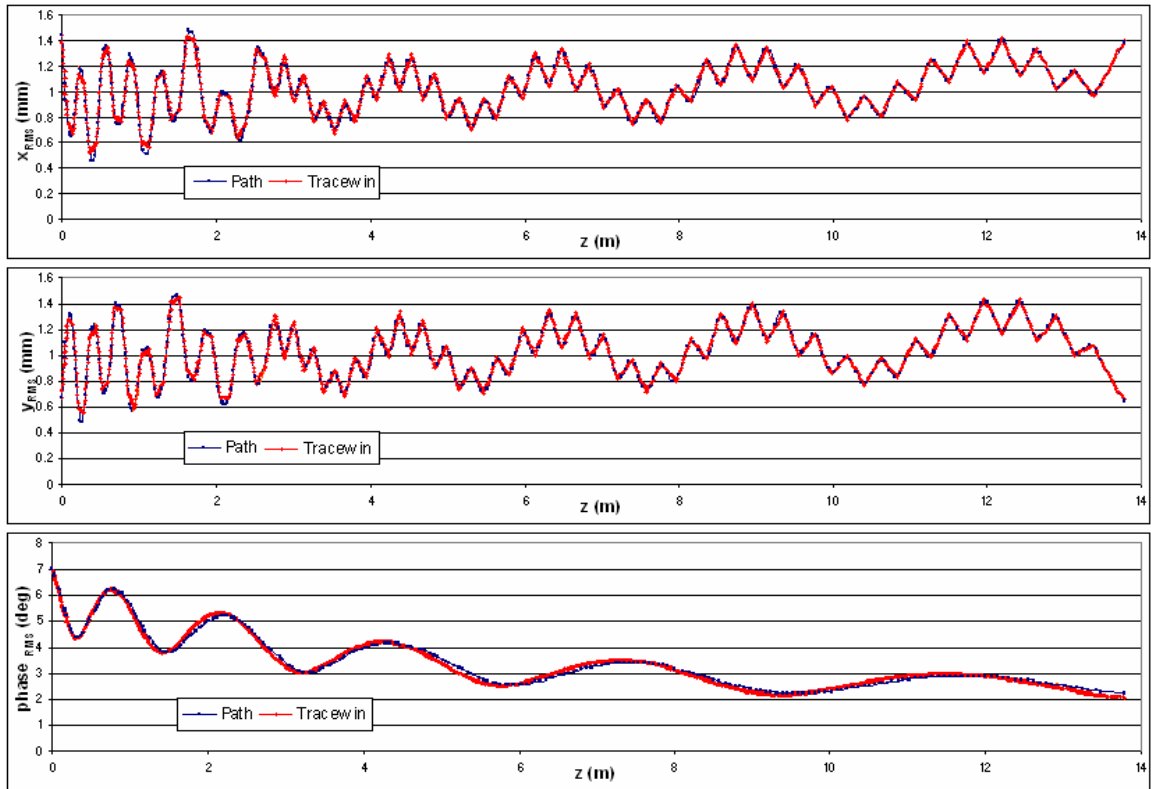


Figure 14: RMS beam size envelopes along the DTL, test beam, $I = 0$ mA

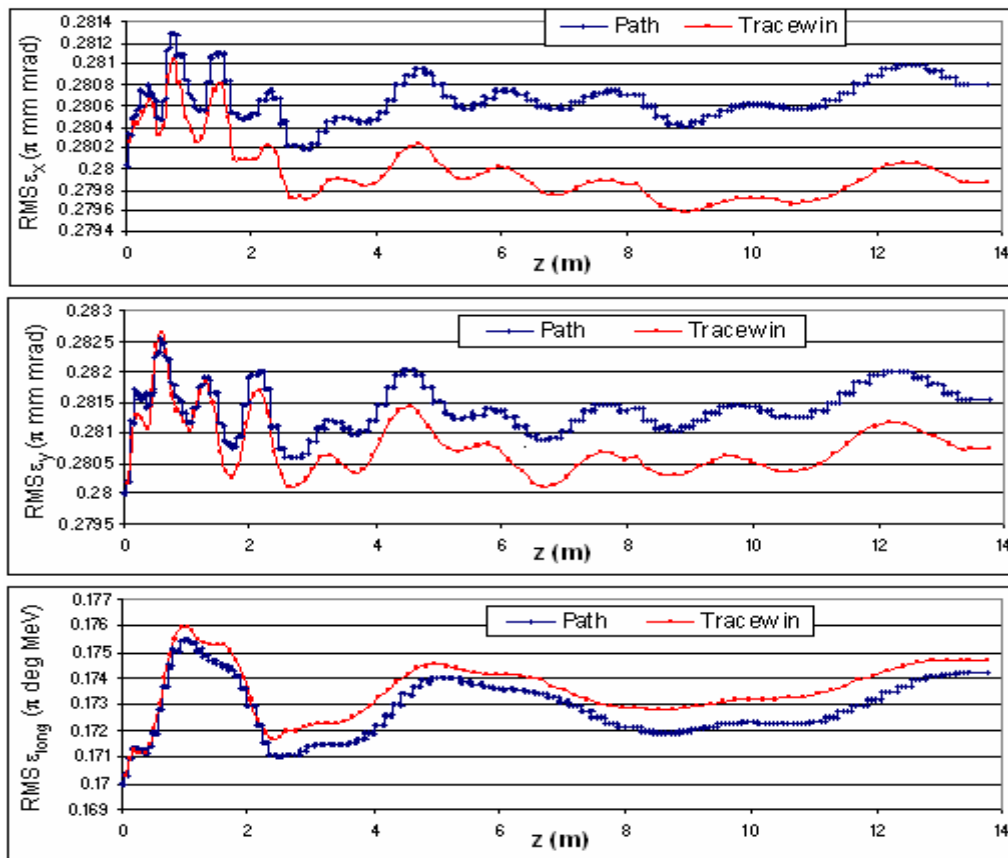


Figure 15: RMS normalized emittance evolution along the DTL, test beam, $I = 0$ mA

The maximum difference between the RMS normalized emittances and RMS beam size envelopes are reported in Table 10 and Table 11 respectively.

Table 10: Maximum difference between the emittances, test beam, I = 0 mA

Max $\Delta\epsilon_x/\epsilon_x$	Max $\Delta\epsilon_y/\epsilon_y$	Max $\Delta\epsilon_{\text{long}}/\epsilon_{\text{long}}$
0.33%	0.29%	0.54%

Table 11: Maximum difference between the RMS beam size envelopes, test beam, I = 0 mA

Max $\Delta x_{\text{RMS}}/x_{\text{RMS}}$	Max $\Delta y_{\text{RMS}}/y_{\text{RMS}}$	Max $\Delta \text{phase}_{\text{RMS}}/\text{phase}_{\text{RMS}}$
21.8%	17.2%	7.1%

The big difference in the values of the RMS beam size envelopes is due to the different ways PATH and TRACEWIN treat the DTL cell: in PATH the DTL cell is modeled as a simple sequence of quadrupoles, drifts and buncher cavities where the only input parameters are the synchronous phase and the effective voltage, whereas in TRACEWIN additional information about the beta, the transit time factor and its derivatives is provided. In fact, if in both codes we model the DTL cell, in this case only the first tank, as it is done in PATH, we obtain the same results, which are presented in Tables 12-13 and Figures 16-17.

Table 12: DTL 1st tank output beam Twiss parameters in TRACEWIN, test beam, I = 0 mA

	α	β	$\epsilon_{\text{RMS},N}$	$\epsilon_{90\%,N}$
x	1.64	0.55 mm/ π mrad	0.28 π mm mrad	1.28 π mm mrad
y	-2.46	0.77 mm/ π mrad	0.28 π mm mrad	1.29 π mm mrad
long	-0.46	102.16 deg/ π MeV	0.17 π deg MeV	0.78 π deg MeV

Table 13: DTL 1st tank output beam Twiss parameters in PATH, test beam, I = 0 mA

	α	β	$\epsilon_{\text{RMS},N}$	$\epsilon_{90\%,N}$
x	1.60	0.55 mm/ π mrad	0.28 π mm mrad	1.27 π mm mrad
y	-2.47	0.77 mm/ π mrad	0.28 π mm mrad	1.28 π mm mrad
long	-0.46	100.08 deg/ π MeV	0.17 π deg MeV	0.77 π deg MeV

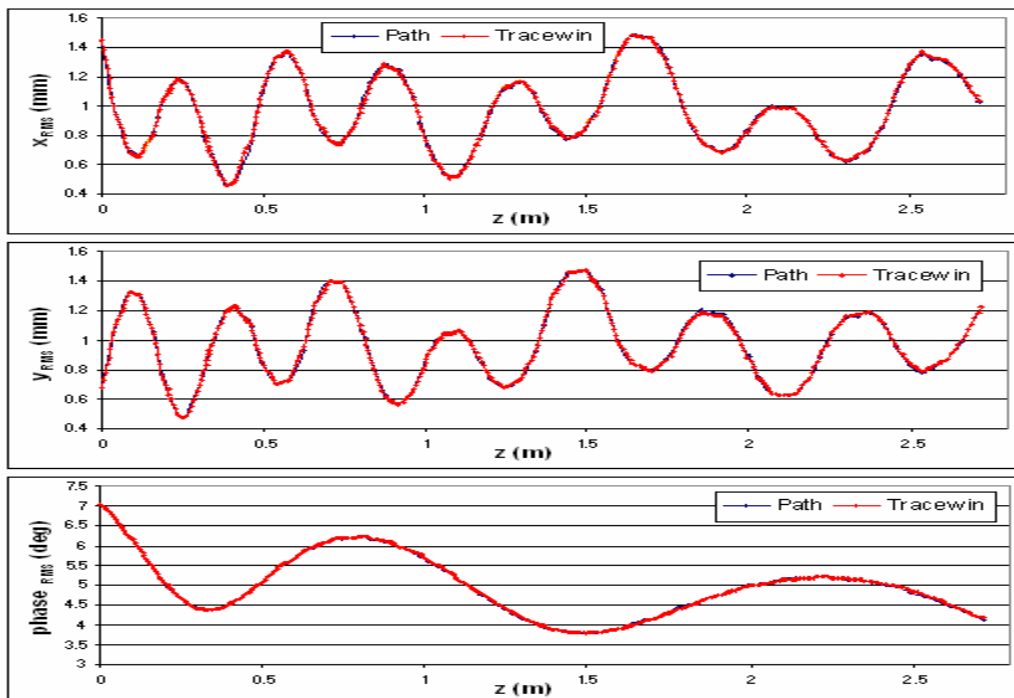


Figure 16: RMS beam size envelopes along the DTL 1st tank, test beam, I = 0 mA

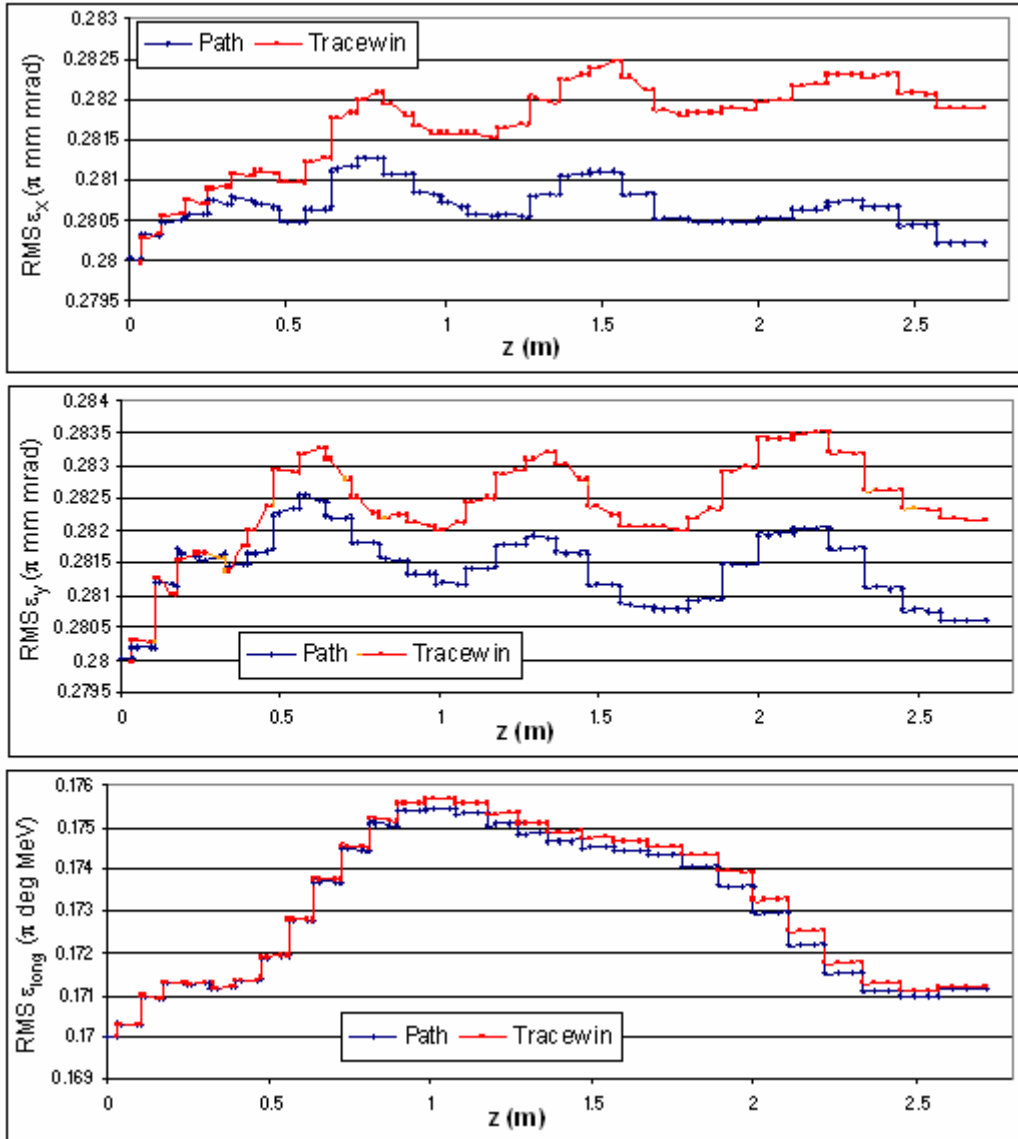


Figure 17: RMS normalized emittances along the DTL 1st tank, test beam, I = 0 mA

The maximum differences between emittances in the two codes are reported in Table 14.

Table 14: Maximum difference between emittances, test beam, I = 0 mA

$\text{Max } \Delta\epsilon_x/\epsilon_x$	$\text{Max } \Delta\epsilon_y/\epsilon_y$	$\text{Max } \Delta\epsilon_{\text{long}}/\epsilon_{\text{long}}$
0.6%	0.5%	0.2%

2.2 Test beam, I = 65 mA

In these simulations a 65 mA current generated input beam was used. The transmission is 100% in both codes. The energy evolution along the DTL is plotted in Figure 18. The output energy is 39.85 MeV in PATH and 39.84 MeV in TRACEWIN.

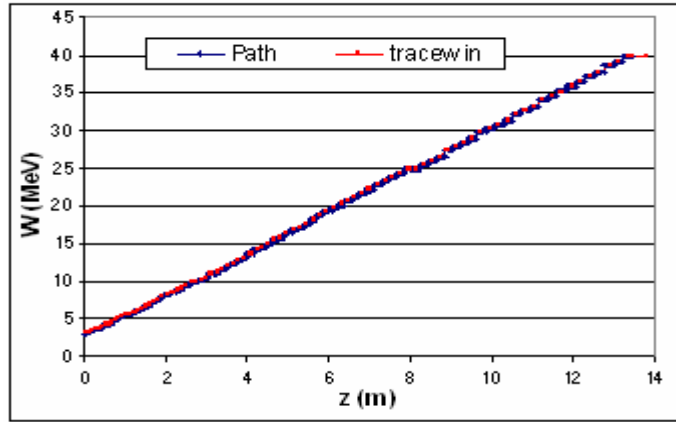


Figure 18: Energy evolution along the DTL, test beam, I = 65 mA

Twiss parameters of the DTL output beam are reported in Table 15 and 16. The output beam phase space is presented in Figures 19 and 20.

Table 15: DTL output beam Twiss parameters in TRACEWIN, test beam, I = 65 mA

	α	β	$\epsilon_{RMS,N}$	$\epsilon_{90\%,N}$
x	-3.03	2.49 mm/ π mrad	0.31 π mm mrad	1.41 π mm mrad
y	2.30	2.39 mm/ π mrad	0.30 π mm mrad	1.38 π mm mrad
long	-0.20	59.74 deg/ π MeV	0.18 π deg MeV	0.81 π deg MeV

Table 16: DTL output beam Twiss parameters in PATH, test beam, I = 65 mA

	α	β	$\epsilon_{RMS,N}$	$\epsilon_{90\%,N}$
x	-2.77	2.36 mm/ π mrad	3.11 π mm mrad	1.41 π mm mrad
y	2.40	2.37 mm/ π mrad	0.30 π mm mrad	1.37 π mm mrad
long	-0.24	63.64 deg/ π MeV	0.18 π deg MeV	0.80 π deg MeV

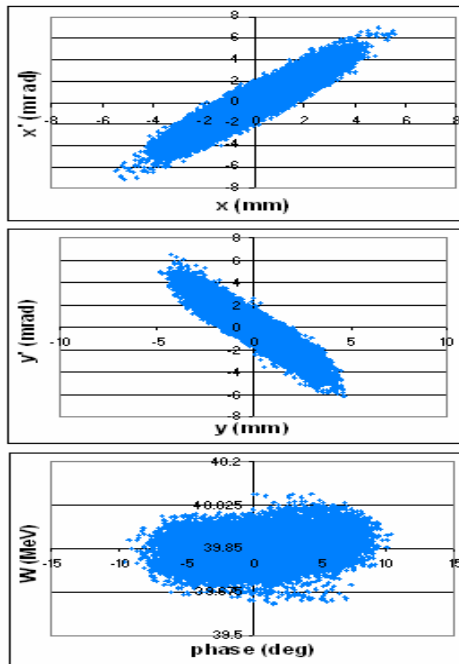


Figure 19: DTL output beam in PATH, test beam, I = 65 mA

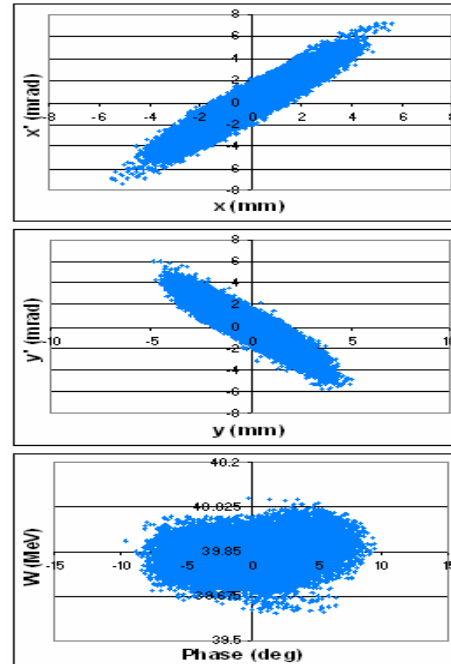


Figure 20: DTL output beam in TRACEWIN, test beam, I = 65 mA

The RMS beam size envelopes and emittances are plotted in Figures 21 and 22.

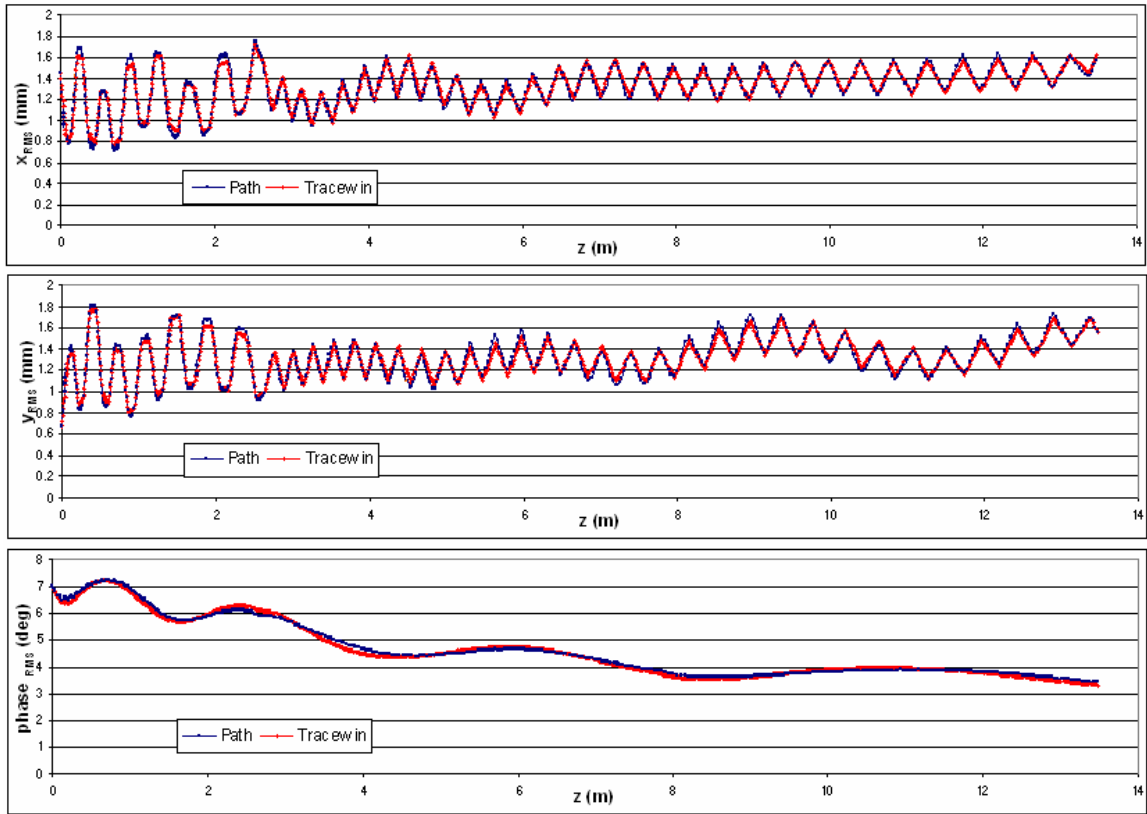


Figure 21: RMS beam size envelopes along the DTL, test beam, $I = 65$ mA

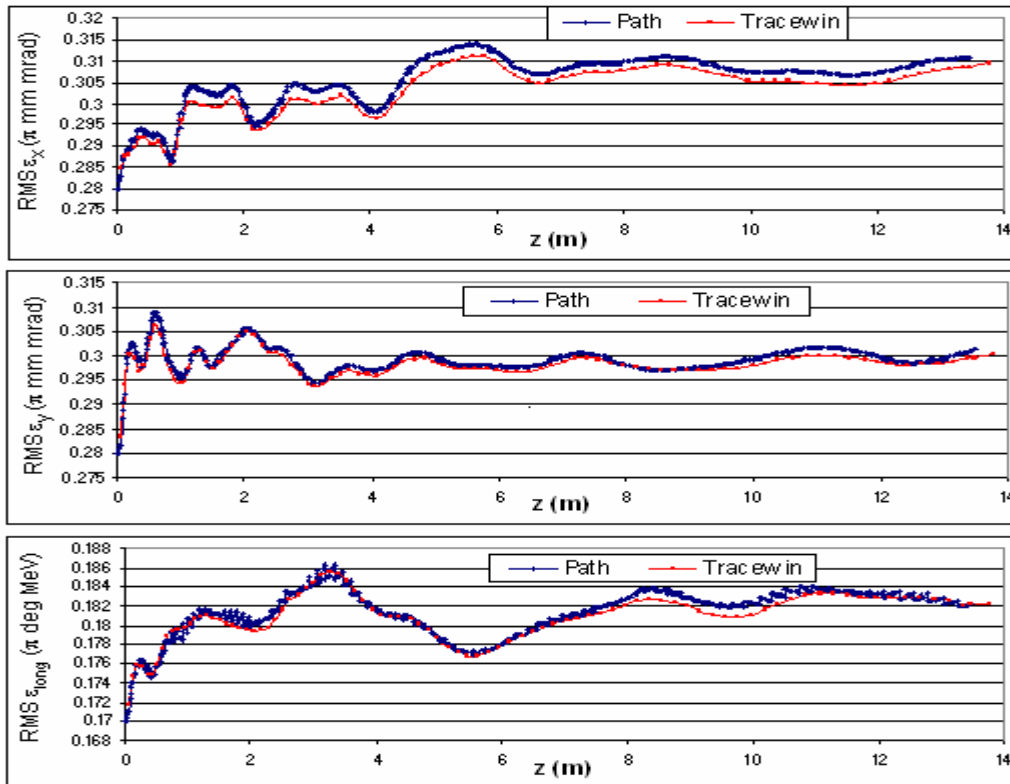


Figure 22: RMS normalized emittance evolution along the DTL, test beam, $I = 65$ mA

Tables 17 and 18 show the relative difference between the RMS envelopes and RMS emittances in the two codes.

Table 17: Maximum difference between the RMS envelopes, test beam, $I = 65$ mA

$\text{Max } \Delta x_{\text{RMS}}/x_{\text{RMS}}$	$\text{Max } \Delta y_{\text{RMS}}/y_{\text{RMS}}$	$\text{Max } \Delta \text{phase}_{\text{RMS}}/\text{phase}_{\text{RMS}}$
5.4%	3.1%	4.6%

Table 18: Maximum difference between the emittances, test beam, $I = 65$ mA

$\text{Max } \Delta \varepsilon_x/\varepsilon_x$	$\text{Max } \Delta \varepsilon_y/\varepsilon_y$	$\text{Max } \Delta \varepsilon_{\text{long}}/\varepsilon_{\text{long}}$
1.30%	1.46%	0.88%

2.3 Beam from Chopper Line, unmatched case ($I = 0$ mA)

In these simulations the Chopper Line output beam with zero current was used at the input of the DTL. The transmission is 99.94% in PATH and 99.95% in TRACEWIN.

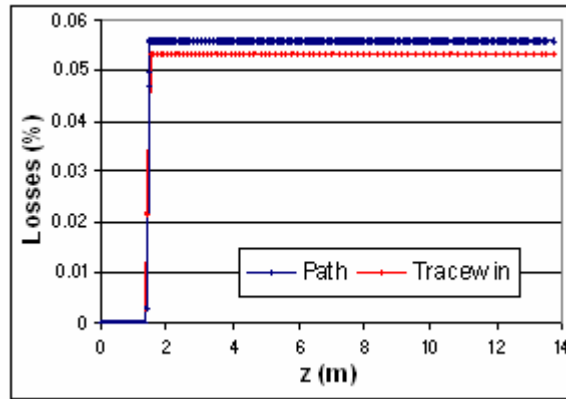


Figure 23: Losses along the DTL, beam from the Chopper Line, unmatched case

The output energy is 40.02 MeV in PATH and 39.84 MeV in TRACEWIN.

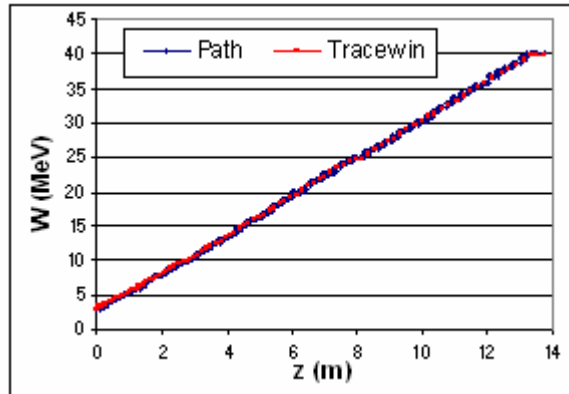


Figure 24: Energy evolution along the DTL, beam from the Chopper, unmatched case

Figures 25 and 26 present the DTL output beam phase space and Twiss parameters are reported in Tables 19 and 20 for TRACEWIN and PATH respectively.

Table 19: DTL output beam Twiss parameters in TRACEWIN, beam from the Chopper Line, unmatched case

	α	β	$\epsilon_{RMS,N}$	$\epsilon_{90\%,N}$
x	-6.69	3.53 mm/ π mrad	0.35 π mm mrad	1.47 π mm mrad
y	5.63	2.32 mm/ π mrad	0.51 π mm mrad	2.40 π mm mrad
long	0.29	42.89 deg/ π MeV	0.17 π deg MeV	0.77 π deg MeV

Table 20: DTL output beam Twiss parameters in PATH, beam from the Chopper Line, unmatched case

	α	β	$\epsilon_{RMS,N}$	$\epsilon_{90\%,N}$
x	-7.23	4.11 mm/ π mrad	0.35 π mm mrad	1.45 π mm mrad
y	4.58	1.74 mm/ π mrad	0.55 π mm mrad	2.52 π mm mrad
long	0.46	37.09 deg/ π MeV	0.17 π deg MeV	0.78 π deg MeV

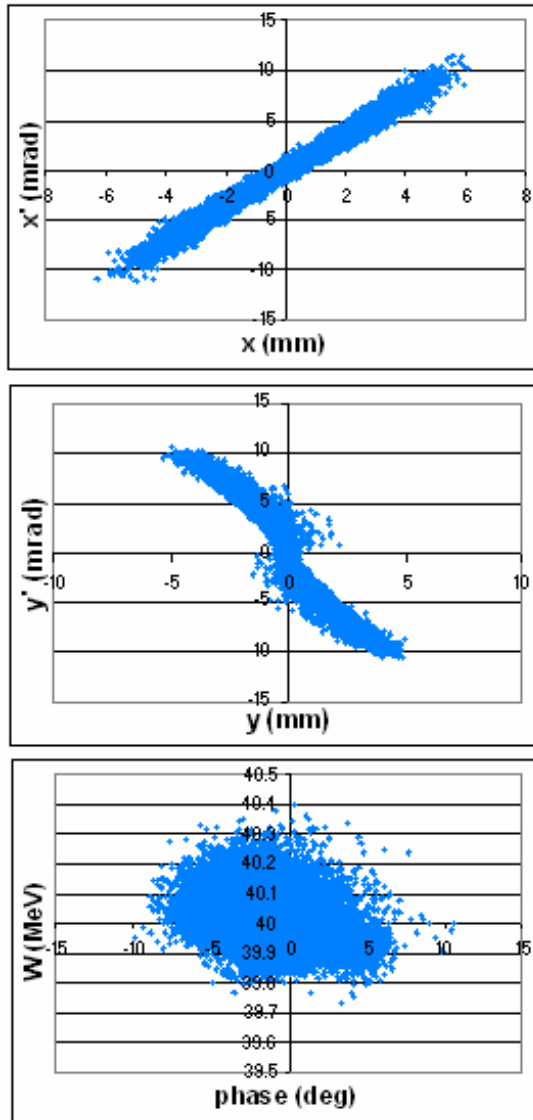


Figure 25: DTL output beam in PATH, beam from the Chopper, unmatched case

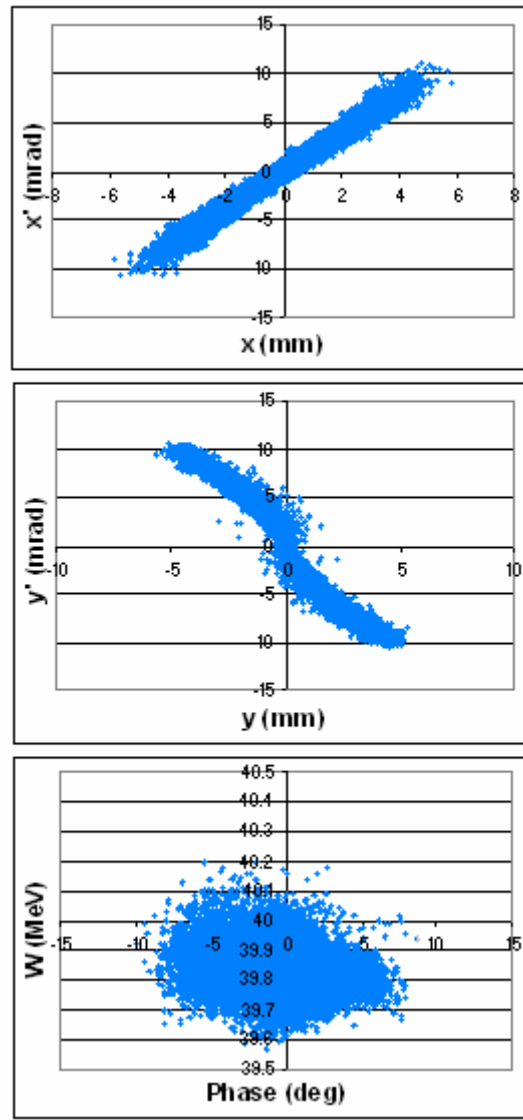


Figure 26: DTL output beam in TRACEWIN, beam from the Chopper, unmatched case

The RMS beam size envelopes and emittances are plotted in Figures 27 and 28.

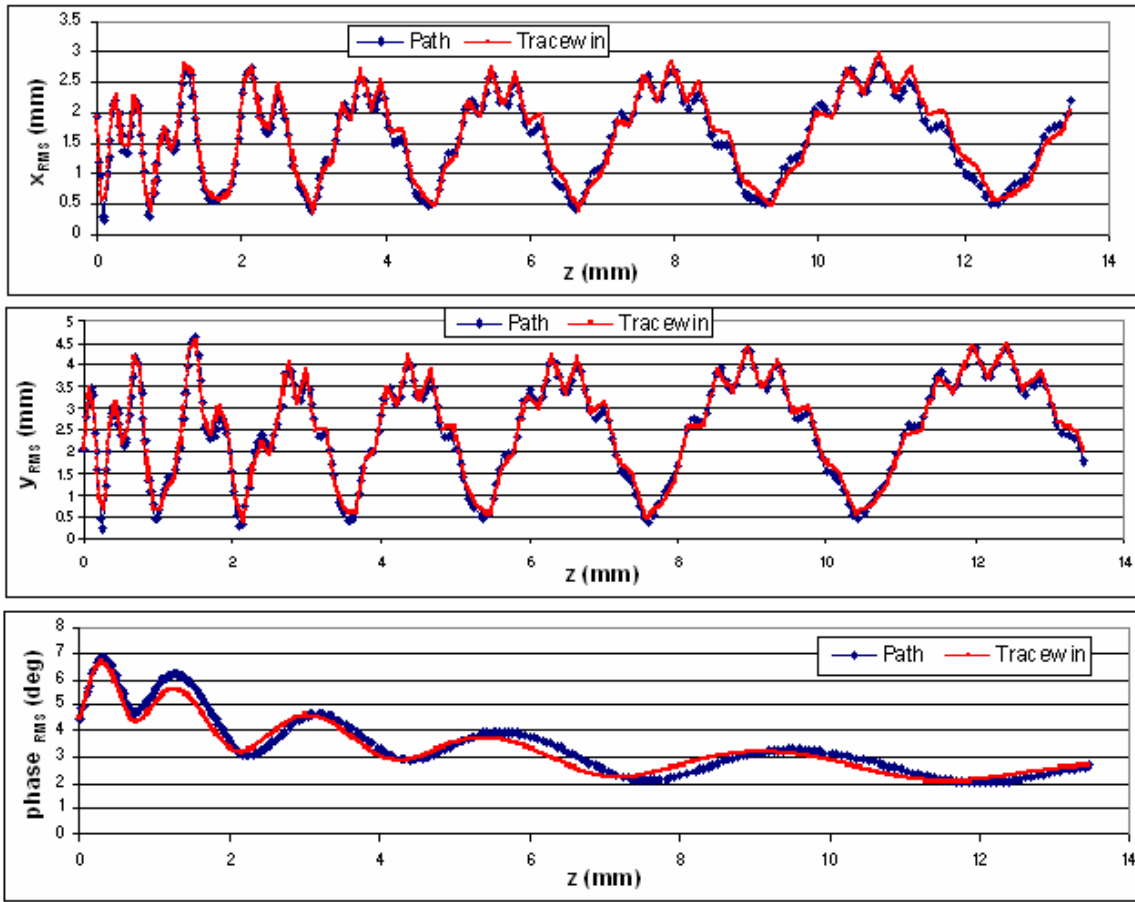


Figure 27: RMS beam size envelopes along the DTL, beam from Chopper, unmatched case

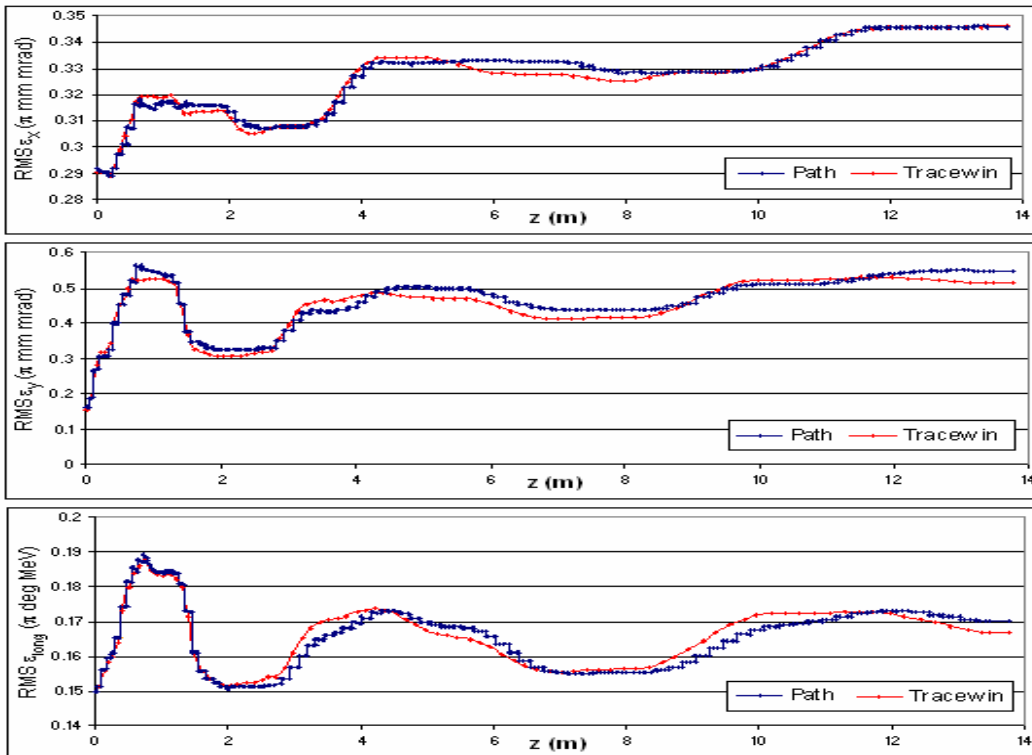


Figure 28: RMS emittances evolution along the DTL, beam from the Chopper, unmatched case

Table 21: Maximum difference between the RMS beam size envelopes, beam from the Chopper Line, unmatched case

$\text{Max } \Delta x_{\text{RMS}}/x_{\text{RMS}}$	$\text{Max } \Delta y_{\text{RMS}}/y_{\text{RMS}}$	$\text{Max } \Delta \text{phase}_{\text{RMS}}/\text{phase}_{\text{RMS}}$
12.2%	33.2%	11.7%

Table 22: Maximum difference between the emittances, beam from the Chopper Line, unmatched case

$\text{Max } \Delta \epsilon_x/\epsilon_x$	$\text{Max } \Delta \epsilon_y/\epsilon_y$	$\text{Max } \Delta \epsilon_{\text{long}}/\epsilon_{\text{long}}$
1.7%	7.4%	4.1%

2.4 Beam from Chopper Line, matched case

In these simulations the Chopper Line output beam with space charge was used. The beam current is 62.2 mA in TRACEWIN and 61.9 mA in PATH, because of the different transmission (88.95% in TRACEWIN and 88.52% in PATH, with an initial current of 69.9 mA) for the Chopper Line in the two codes.

The transmission in the DTL is 100% in both codes (just one lost particle on 44201 in the middle of the first tank). The output energy is 39.85 MeV in PATH and 39.84 MeV in TRACEWIN.

Figures 29 and 30 present the DTL output beams and their Twiss parameters are reported in Tables 23 and 24, obtained with TRACEWIN and PATH respectively.

Table 23: DTL output beam Twiss parameters in TRACEWIN, beam from Chopper, I = 62 mA

	α	β	$\epsilon_{\text{RMS},N}$	$\epsilon_{90\%,N}$
x	-2.89	2.52 mm/ π mrad	0.34 π mm mrad	1.46 π mm mrad
y	2.28	2.12 mm/ π mrad	0.32 π mm mrad	1.35 π mm mrad
long	0.11	56.08 deg/ π MeV	0.18 π deg MeV	0.87 π deg MeV

Table 24: DTL output beam Twiss parameters in PATH, beam from Chopper, I = 62 mA

	α	β	$\epsilon_{\text{RMS},N}$	$\epsilon_{90\%,N}$
x	-2.65	2.35 mm/ π mrad	0.35 π mm mrad	1.48 π mm mrad
y	2.24	2.03 mm/ π mrad	0.33 π mm mrad	1.35 π mm mrad
long	0.08	56.03 deg/ π MeV	0.18 π deg MeV	0.86 π deg MeV

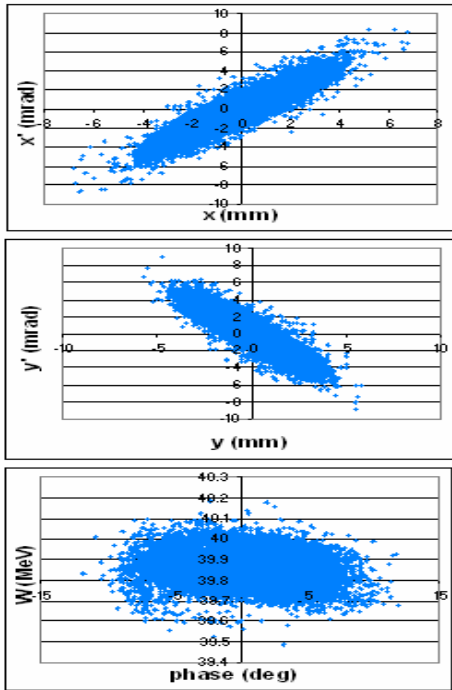


Figure 29: DTL output beam in PATH, beam from the Chopper, I = 62 mA

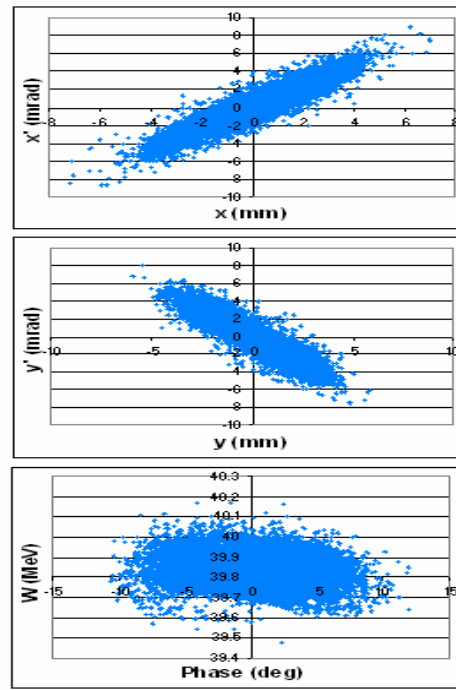


Figure 30: DTL output beam in TRACEWIN, beam from the Chopper, I = 62 mA

The RMS beam size envelopes and emittances are plotted in Figures 31 and 32.

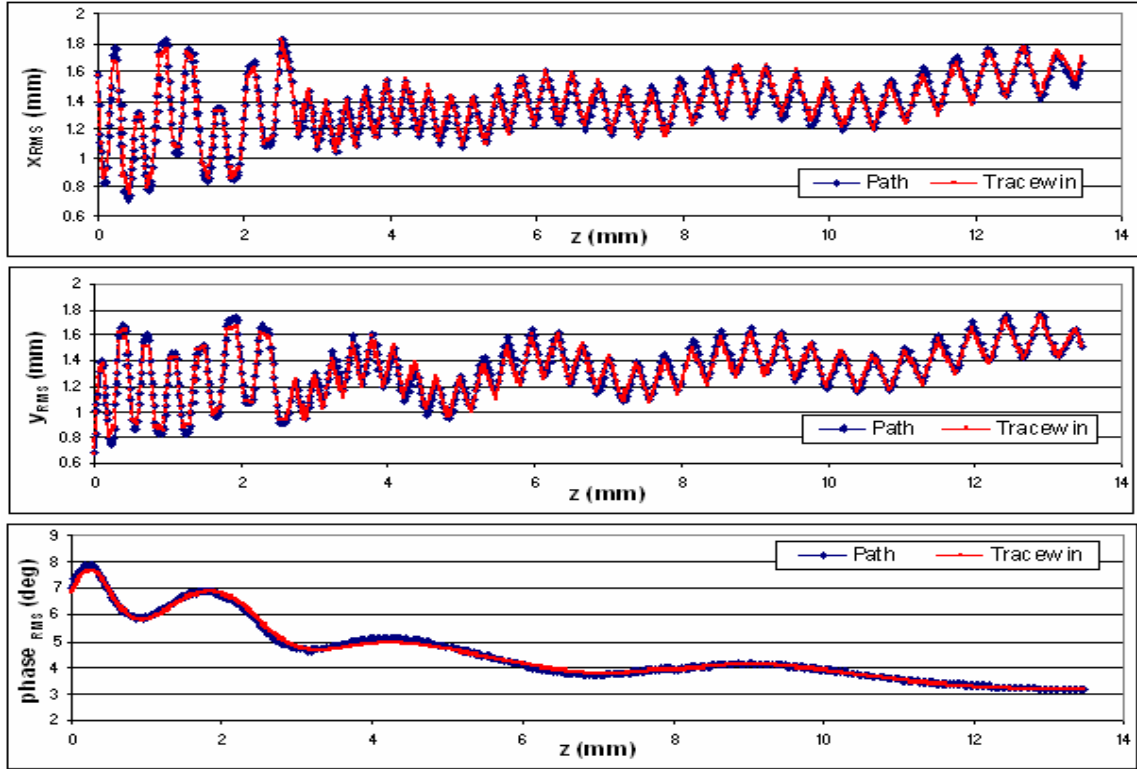


Figure 31: RMS beam size envelopes along the DTL, beam from the Chopper Line, $I = 62$ mA

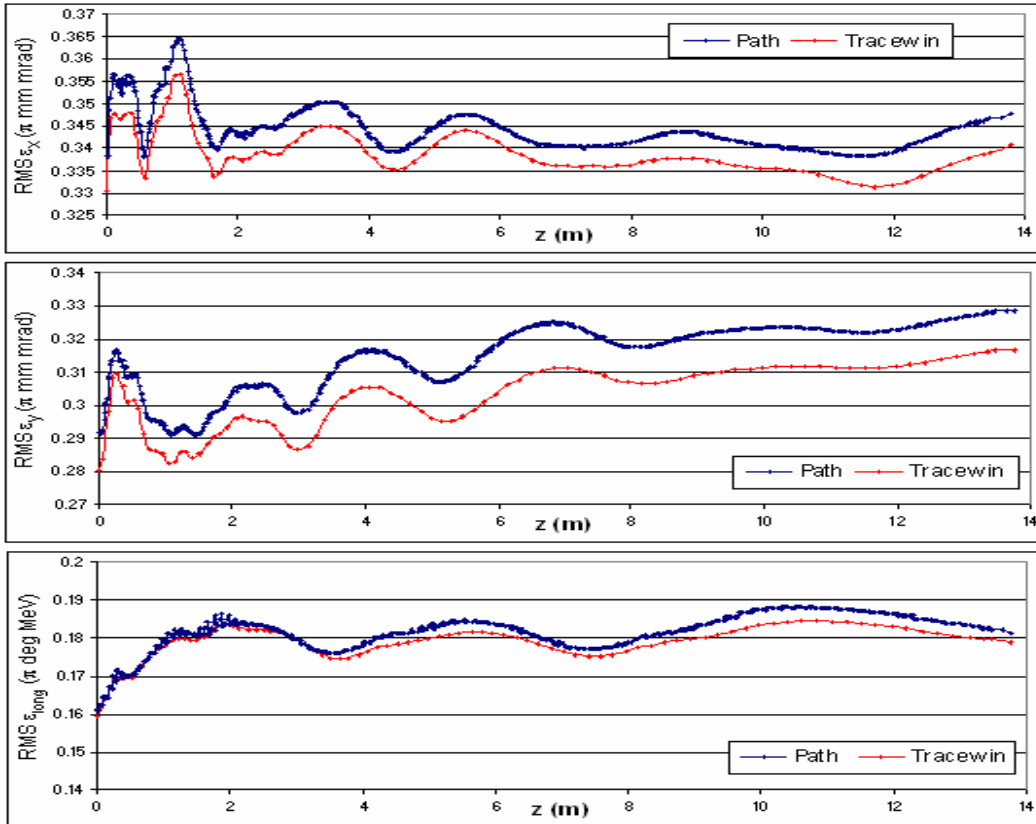


Figure 32: RMS emittances along the DTL, beam from the Chopper, $I = 62$ mA

Table 25: Maximum difference between the RMS beam size envelopes, beam from the Chopper Line,
I = 62 mA

Max $\Delta x_{RMS}/x_{RMS}$	Max $\Delta y_{RMS}/y_{RMS}$	Max $\Delta \text{phase}_{RMS}/\text{phase}_{RMS}$
4.7%	10%	3.2%

Table 26: Maximum difference between the emittances, beam from the Chopper Line, I = 62 mA

Max $\Delta \epsilon_x/\epsilon_x$	Max $\Delta \epsilon_y/\epsilon_y$	Max $\Delta \epsilon_{long}/\epsilon_{long}$
2.4%	4.4%	2.1%

The RMS and 90% emittance growth in the DTL is reported in Tables 27 and 28.

Table 27: RMS emittance growth in the DTL

	ϵ_x	ϵ_y	ϵ_{long}
PATH	2.4%	12.6%	13.3%
TRACEWIN	2.5%	12.8%	12.6%

Table 28: 90% emittance growth in the DTL

	ϵ_x	ϵ_y	ϵ_{long}
PATH	3.7%	2.8%	18.4%
TRACEWIN	4.7%	7.4%	18.2%

2.5 Summary of Section 2

The envelopes of the beam characteristics obtained with the PATH and TRACEWIN are quite similar, both without and with space charge effects.

The differences are due mainly to the different ways the two codes treat the DTL cell.

With the space charge the agreement between the codes is better than the 0 mA current one, so this effect is somehow overridden by the space charge effects.

3. Beam dynamics in the CCDTL

As in the previous sections, in order to check the structure the first simulation has been done without space-charge effects and with a test beam generated at the input of the CCDTL. Further, the beam coming from the DTL has been used for simulations with and without space-charge.

3.1 Test beam, I = 0 mA

The characteristics of the generated input beam are:

- Number of particles = 44670
- $f = 352.2$ MHz
- $E_{in} = 39.8364$ MeV
- Twiss parameters:

	α	β	$\epsilon_{RMS,N}$
x	-4.36	4.55 mm/ π mrad	0.33 π mm mrad
y	1.12	1.10 mm/ π mrad	0.32 π mm mrad
long	0.38	60.63 deg/ π MeV	0.17 π deg MeV

Without space charge effects, the transmission is 99.996% with both codes. The evolution of losses is plotted in Figure 33.

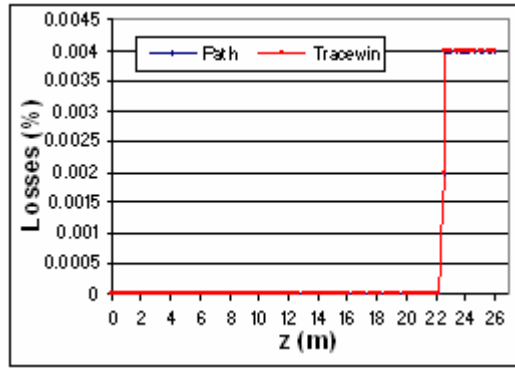


Figure 33: Losses along the CCDTL, test beam, $I = 0$ mA

The energy evolution is plotted in Figure 34. The final energies are, respectively, 89.670 MeV in PATH and 89.685 MeV in TRACEWIN.

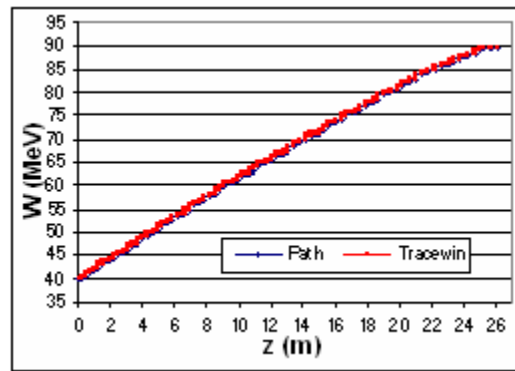


Figure 34: Energy evolution along the CCDTL, test beam, $I = 0$ mA

The CCDTL output beam shapes are plotted in Figures 35 and 36. Twiss parameters are reported in Tables 29 and 30.

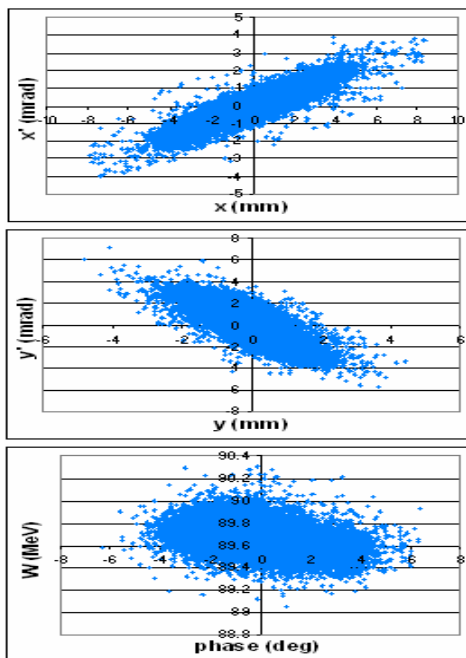


Figure 35: CCDTL output beam in PATH, test beam, $I = 0$ mA

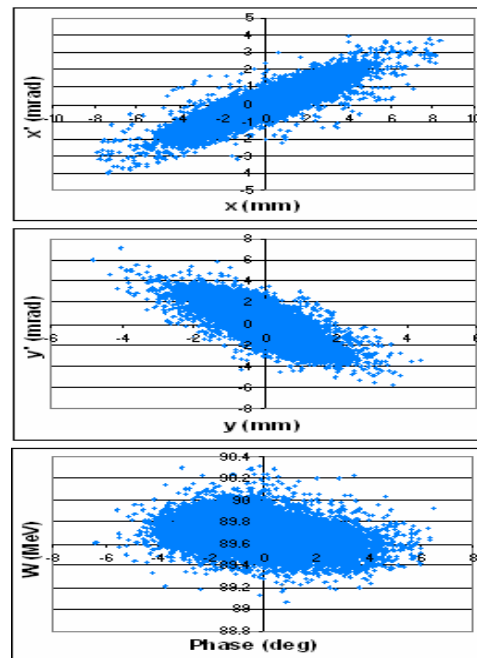


Figure 36: CCDTL output beam in TRACEWIN, test beam, $I = 0$ mA

Table 29: CCDTL output beam Twiss parameters in TRACEWIN, test beam, I = 0 mA

	α	β	$\epsilon_{RMS,N}$	$\epsilon_{90\%,N}$
x	-2.07	5.11 mm/ π mrad	0.33 π mm mrad	1.38 π mm mrad
y	1.47	1.09 mm/ π mrad	0.32 π mm mrad	1.32 π mm mrad
long	0.49	16.93 deg/ π MeV	0.17 π deg MeV	0.79 π deg MeV

Table 30: CCDTL output beam Twiss parameters in PATH, test beam, I = 0 mA

	α	β	$\epsilon_{RMS,N}$	$\epsilon_{90\%,N}$
x	-2.10	5.15 mm/ π mrad	0.33 π mm mrad	1.33 π mm mrad
y	1.48	1.11 mm/ π mrad	0.32 π mm mrad	1.30 π mm mrad
long	0.49	16.87 deg/ π MeV	0.17 π deg MeV	0.78 π deg MeV

The RMS envelopes and emittances are plotted in Figures 37 and 38.

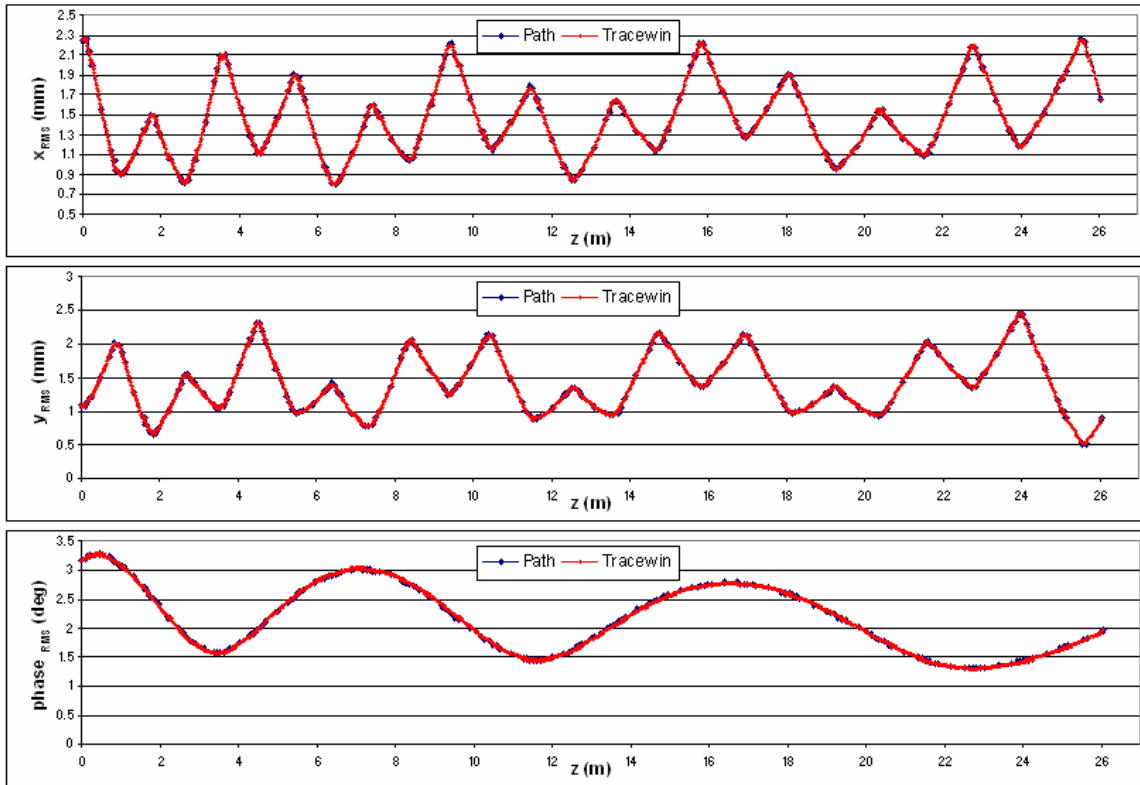


Figure 37: RMS beam size envelopes along the CCDTL, test beam, I = 0 mA

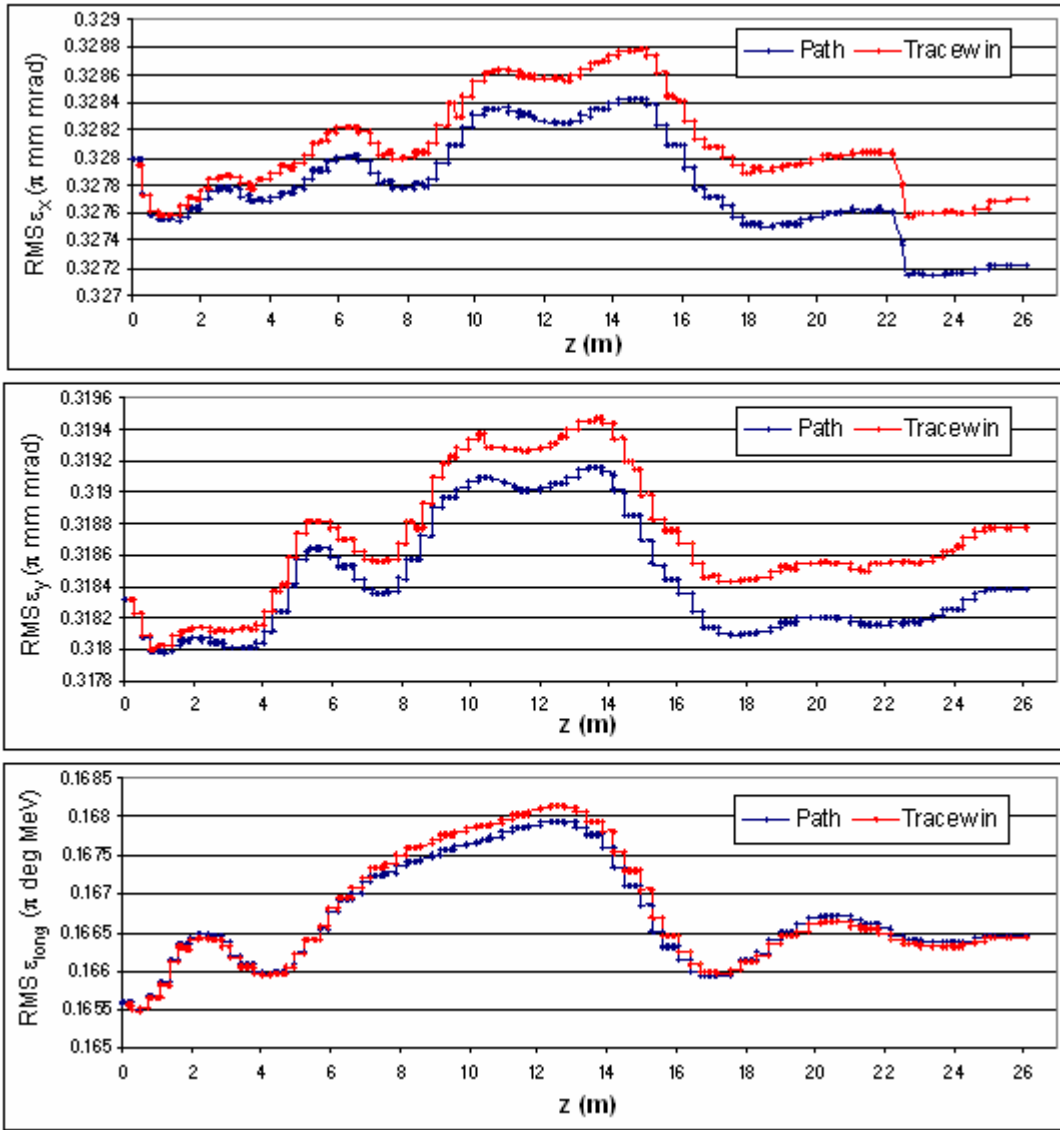


Figure 38: RMS normalized emittance evolution along the CCDTL, test beam, $I = 0$ mA

In Table 31 the maximum difference between emittances in the two codes are reported, taking the TRACEWIN results as reference ($(X_{\text{PATH}} - X_{\text{TRACEWIN}}) / X_{\text{TRACEWIN}}$).

Table 31: Maximum difference between the emittances, test beam, $I = 0$ mA

Max $\Delta\epsilon_x/\epsilon_x$	Max $\Delta\epsilon_y/\epsilon_y$	Max $\Delta\epsilon_{\text{long}}/\epsilon_{\text{long}}$
-0.15%	-0.12%	-0.12%

3.2 Test beam, $I = 65$ mA

In the simulations with space-charge, the transmission is 100% in both codes. The energy evolution is plotted in Figure 39. The final energy is the same as in the case without space charge in TRACEWIN (89.69 MeV), but it has changed in PATH (89.69 MeV).

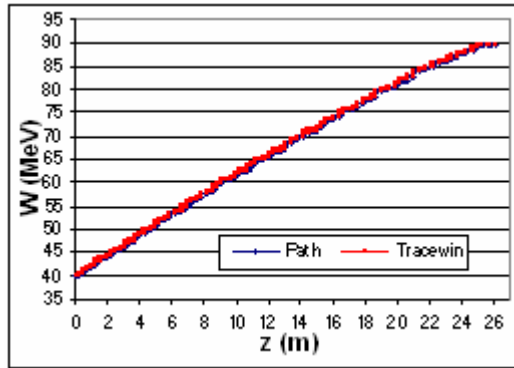


Figure 39: Energy evolution along the CCDTL, test beam, I = 65 mA

The CCDTL output beam shapes are presented in Figures 40 and 41. Twiss parameters are reported in Tables 32 and 33, obtained respectively with TRACEWIN and PATH.

Table 32: CCDTL output beam Twiss parameters in TRACEWIN, test beam, I = 65 mA

	α	β	$\epsilon_{RMS,N}$	$\epsilon_{90\%,N}$
x	-3.01	6.78 mm/ π mrad	0.32 π mm mrad	1.35 π mm mrad
y	1.44	1.75 mm/ π mrad	0.33 π mm mrad	1.36 π mm mrad
long	-0.61	26.33 deg/ π MeV	0.17 π deg MeV	0.78 π deg MeV

Table 33: CCDTL output beam Twiss parameters in PATH, test beam, I = 65 mA

	α	β	$\epsilon_{RMS,N}$	$\epsilon_{90\%,N}$
x	-3.09	2.36 mm/ π mrad	3.13 π mm mrad	1.33 π mm mrad
y	1.47	2.37 mm/ π mrad	0.33 π mm mrad	1.31 π mm mrad
long	-0.58	25.05 deg/ π MeV	0.17 π deg MeV	0.76 π deg MeV

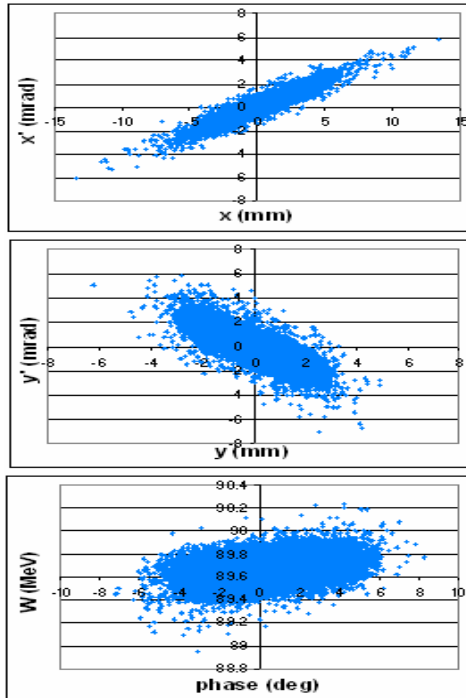


Figure 40: CCDTL output beam in PATH, test beam, I = 65 mA

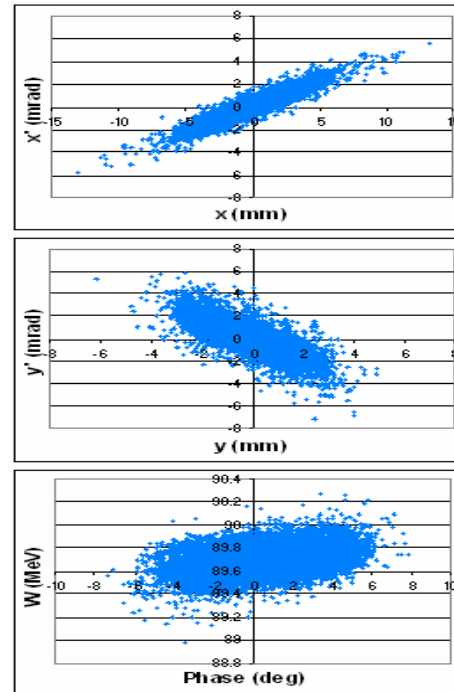


Figure 41: CCDTL output beam in TRACEWIN, test beam, I = 65 mA

The RMS envelopes and emittances are plotted in Figures 42 and 43.

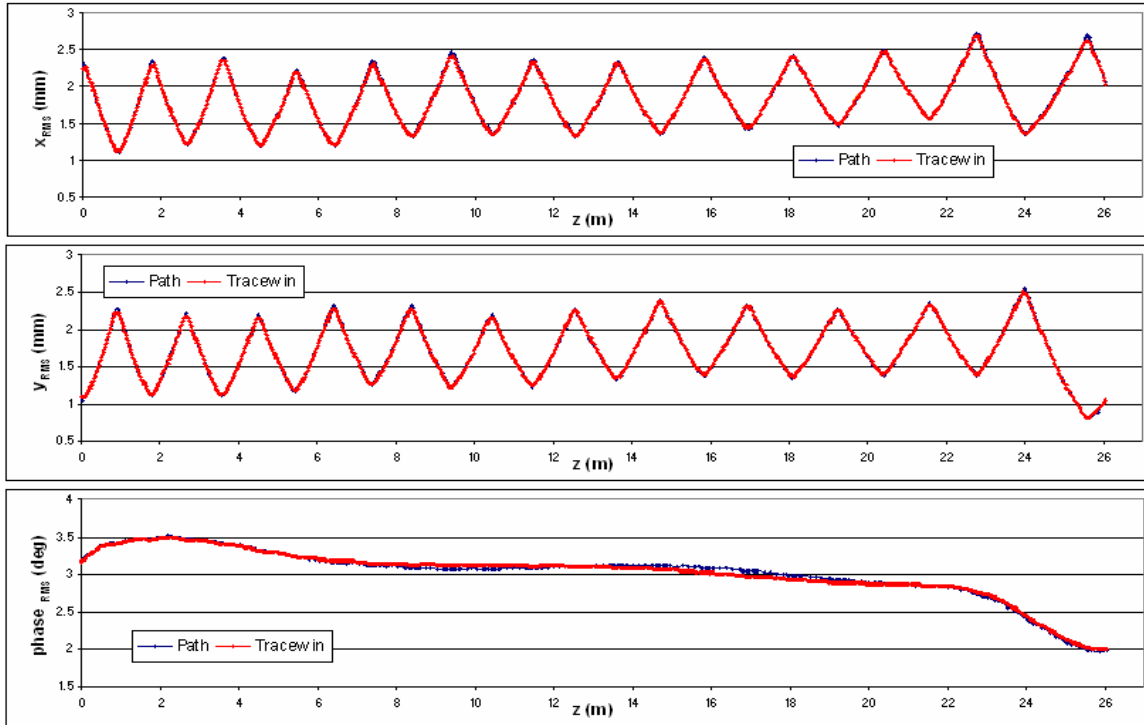


Figure 42: RMS beam size envelopes along the CCDTL, test beam, $I = 65$ mA

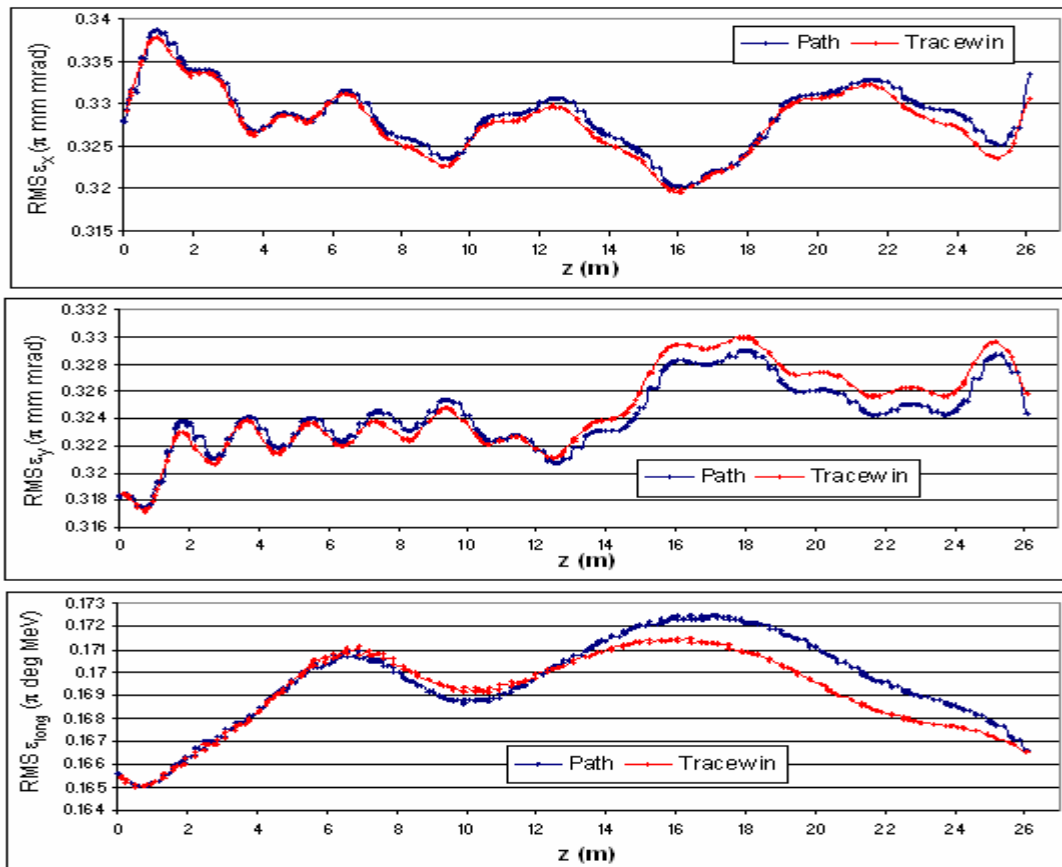


Figure 43: RMS normalized emittance along the CCDTL, test beam, $I = 65$ mA

Table 34: Maximum difference between the RMS envelopes, test beam, I = 65 mA

Max $\Delta x_{RMS}/x_{RMS}$	Max $\Delta y_{RMS}/y_{RMS}$	Max $\Delta \text{phase}_{RMS}/\text{phase}_{RMS}$
2.8%	2.7%	2.3%

Table 35: Maximum difference between the emittances, test beam, I = 65 mA

Max $\Delta \epsilon_x/\epsilon_x$	Max $\Delta \epsilon_y/\epsilon_y$	Max $\Delta \epsilon_{\text{long}}/\epsilon_{\text{long}}$
0.5%	-0.4%	0.9%

3.3 Beam from the DTL, unmatched case (I = 0 mA)

The transmission is 100% in both codes. The final energy is 89.92 MeV in PATH and 89.69 MeV in TRACEWIN.

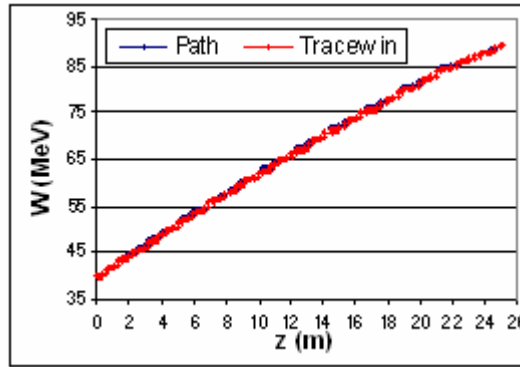


Figure 44: Energy evolution along the CCDTL, beam from the DTL, unmatched case

The CCDTL output beam shapes are represented in Figures 45 and 46. Twiss parameters are reported in Tables 36 and 37, obtained respectively with TRACEWIN and PATH.

Table 36: CCDTL output beam Twiss parameters in TRACEWIN, beam from the DTL, unmatched case

	α	β	$\epsilon_{RMS,N}$	$\epsilon_{90\%,N}$
x	-8.55	15.33 mm/ π mrad	0.35 π mm mrad	1.48 π mm mrad
y	-0.86	3.43 mm/ π mrad	0.51 π mm mrad	2.30 π mm mrad
long	0.36	13.27 deg/ π MeV	0.16 π deg MeV	0.74 π deg MeV

Table 37: CCDTL output beam Twiss parameters in PATH, beam from the DTL, unmatched case

	α	β	$\epsilon_{RMS,N}$	$\epsilon_{90\%,N}$
x	-7.91	14.99 mm/ π mrad	0.35 π mm mrad	1.47 π mm mrad
y	-0.60	3.61 mm/ π mrad	0.54 π mm mrad	2.42 π mm mrad
long	0.31	9.22 deg/ π MeV	0.16 π deg MeV	0.73 π deg MeV

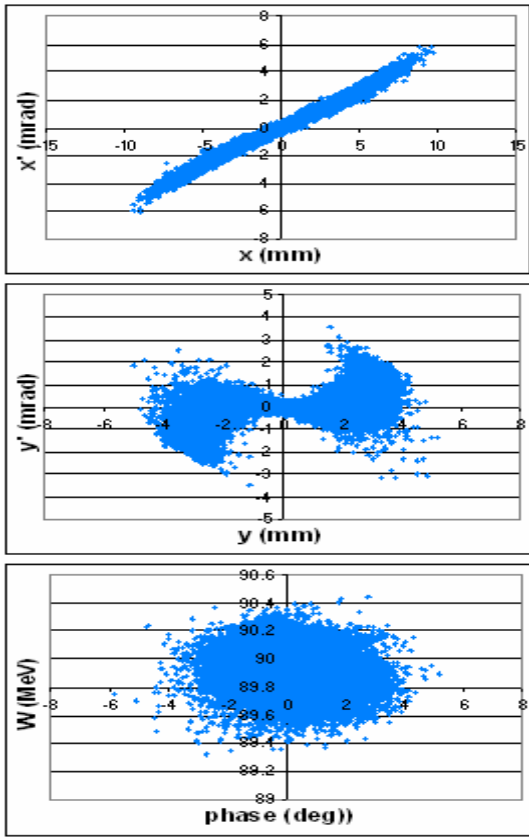


Figure 45: DTL output beam in PATH, beam from the DTL, unmatched case

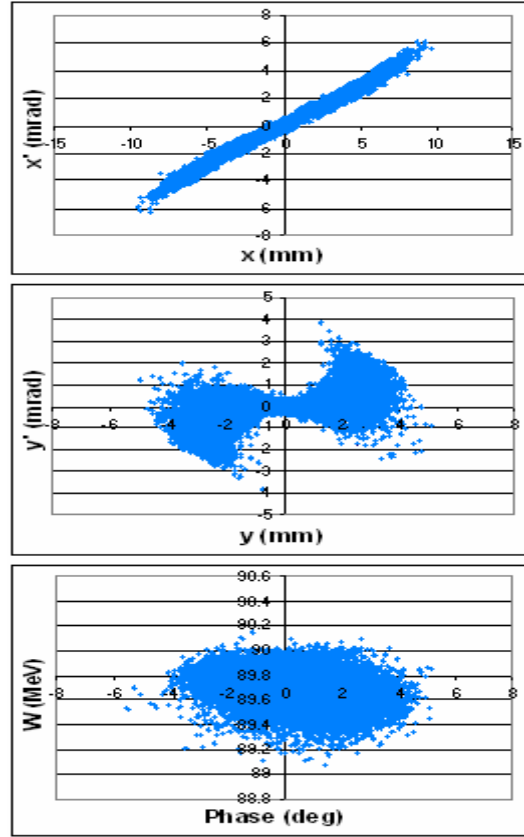


Figure 46: CCDTL output beam in TRACEWIN, TRACEWIN from the DTL, unmatched case

The RMS beam size envelopes and emittances are plotted in Figures 47 and 48.

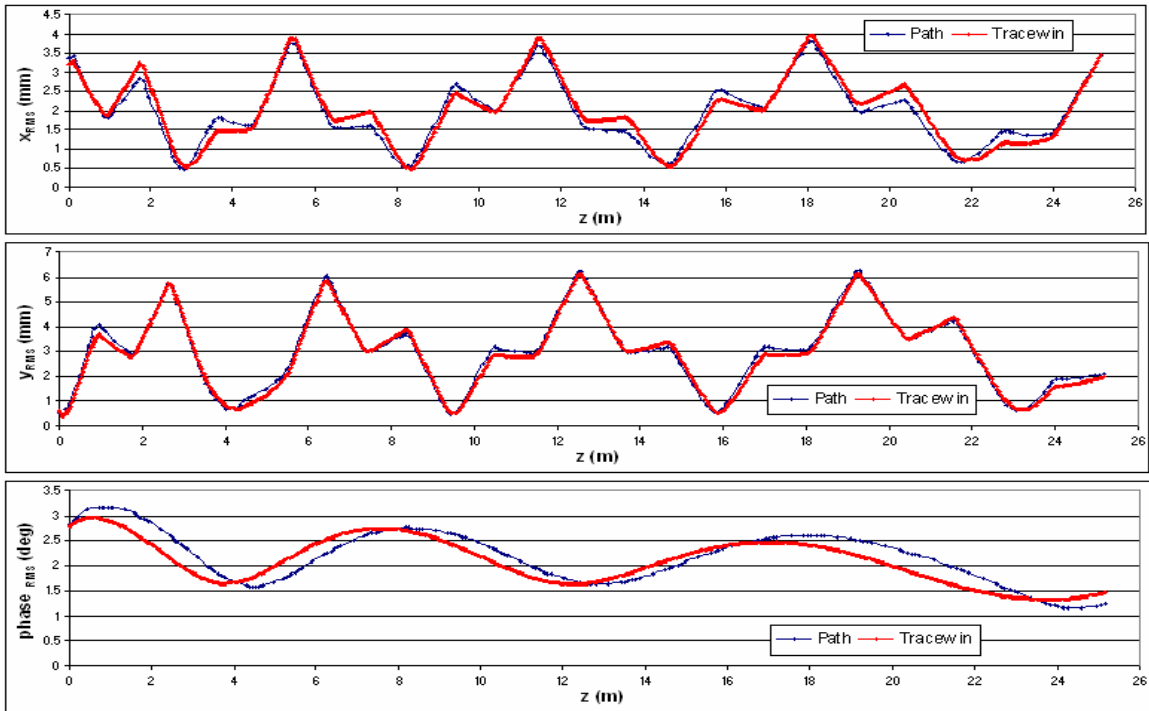


Figure 47: RMS beam size envelopes along the CCDTL, beam from the DTL, unmatched case

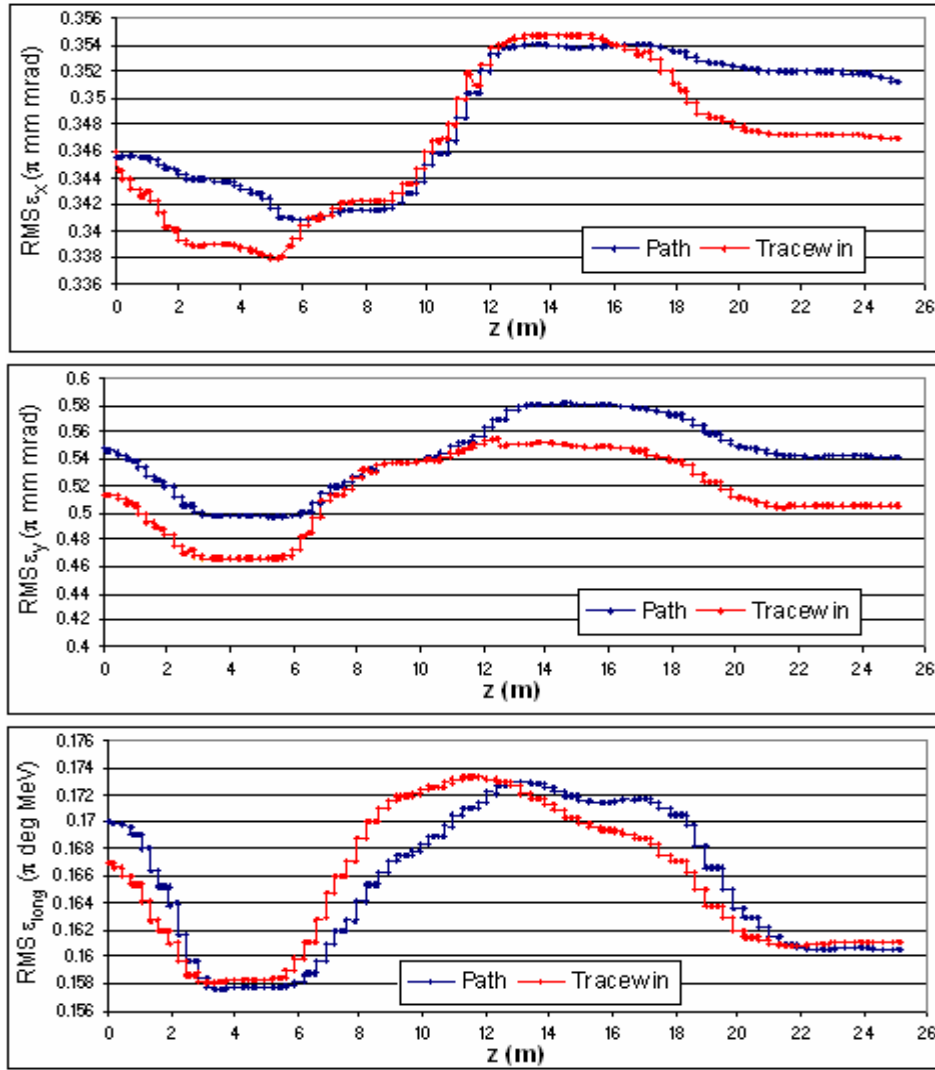


Figure 48: RMS emittances along the CCDTL, beam from the DTL, unmatched case

Table 38: Maximum difference between the RMS beam size, beam from the DTL, unmatched case

$\text{Max } \Delta x_{\text{RMS}}/x_{\text{RMS}}$	$\text{Max } \Delta y_{\text{RMS}}/y_{\text{RMS}}$	$\text{Max } \Delta \text{phase}_{\text{RMS}}/\text{phase}_{\text{RMS}}$
17.5%	15.5%	21.9%

Table 39: Maximum difference between the emittances, beam from the DTL, unmatched case

$\text{Max } \Delta \epsilon_x/\epsilon_x$	$\text{Max } \Delta \epsilon_y/\epsilon_y$	$\text{Max } \Delta \epsilon_{\text{long}}/\epsilon_{\text{long}}$
1.4%	7.7%	-2.4%

3.4 Beam from the DTL, matched case

The beam current is 62.2 mA in TRACEWIN and 61.9 mA in PATH, because of the different transmissions in the Chopper Line with the two codes. The transmission in CCDTL is 100%. The final energy is 89.67 MeV in PATH and 89.69 MeV in TRACEWIN. The two codes agree within 0.03%. The CCDTL output beam shapes are plotted in Figures 49 and 50. Twiss parameters are reported in Tables 40 and 41, respectively for TRACEWIN and PATH.

Table 40: CCDTL output beam Twiss parameters in TRACEWIN, beam from DTL, I = 62 mA

	α	β	$\epsilon_{RMS,N}$	$\epsilon_{90\%,N}$
x	-3.02	6.63 mm/ π mrad	0.34 π mm mrad	1.47 π mm mrad
y	1.39	1.77 mm/ π mrad	0.32 π mm mrad	1.38 π mm mrad
long	-0.53	26.58 deg/ π MeV	0.18 π deg MeV	0.85 π deg MeV

Table 41: CCDTL output beam Twiss parameters in PATH, beam from DTL, I = 62 mA

	α	β	$\epsilon_{RMS,N}$	$\epsilon_{90\%,N}$
x	-3.07	6.77 mm/ π mrad	0.35 π mm mrad	1.45 π mm mrad
y	1.47	1.82 mm/ π mrad	0.33 π mm mrad	1.37 π mm mrad
long	-0.54	25.45 deg/ π MeV	0.18 π deg MeV	0.85 π deg MeV

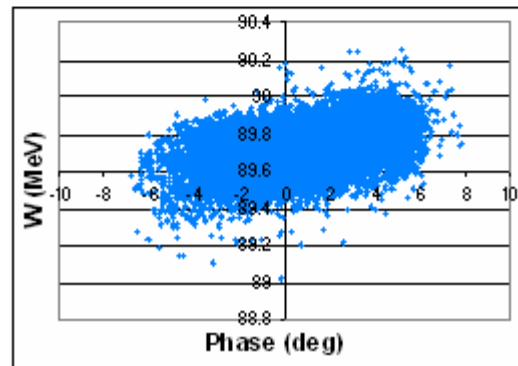
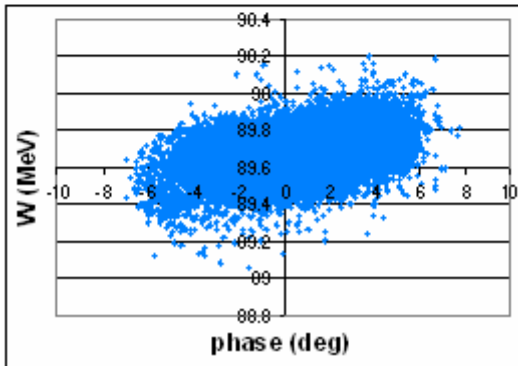
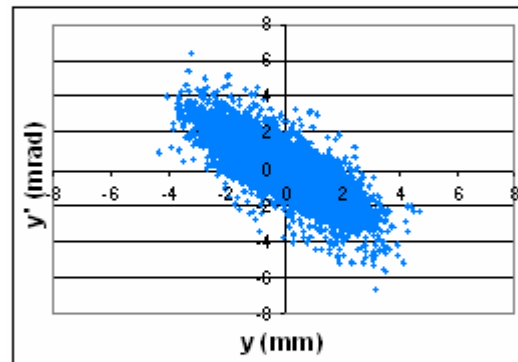
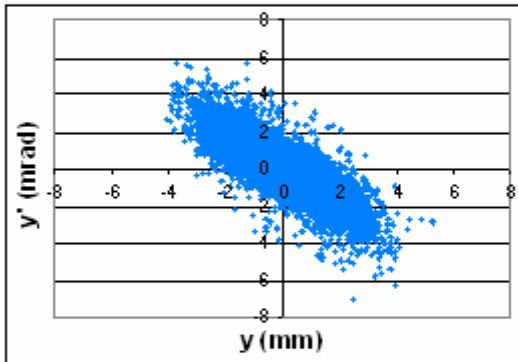
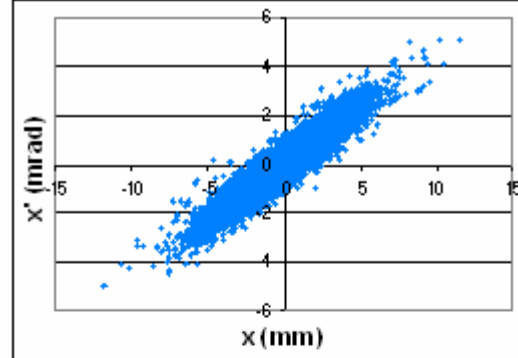
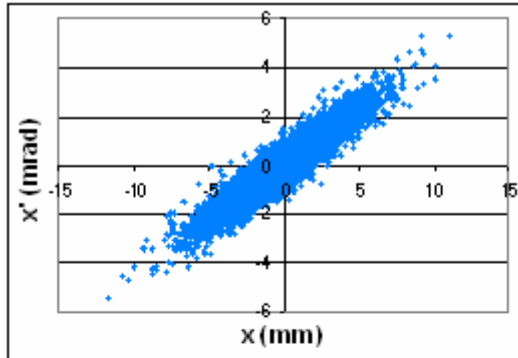


Figure 49: CCDTL output beam in PATH, beam from the DTL, I = 62 mA

Figure 50: CCDTL output beam in TRACEWIN, beam from the DTL, I = 62 mA

The RMS beam size envelopes and emittances along the CCDTL are plotted in Figures 51 and 52.

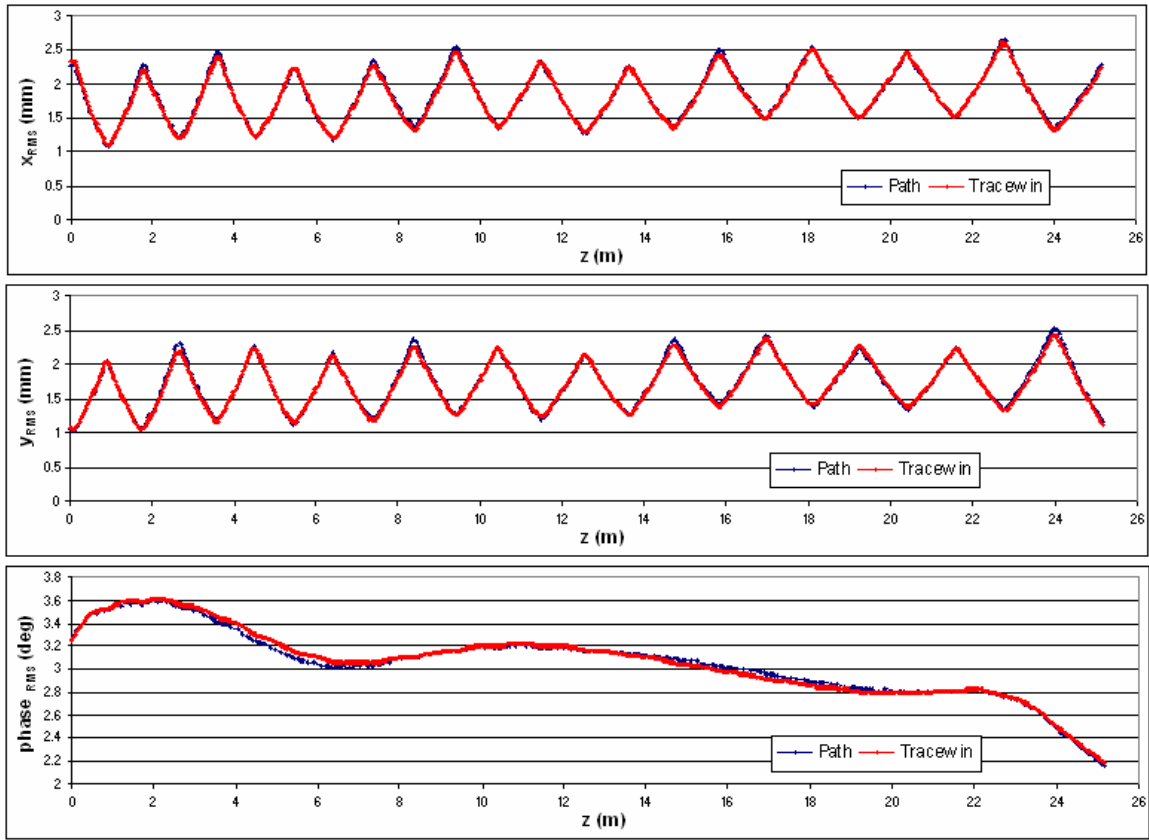


Figure 51: RMS beam size along the CCDTL, beam from the DTL, $I = 62$ mA

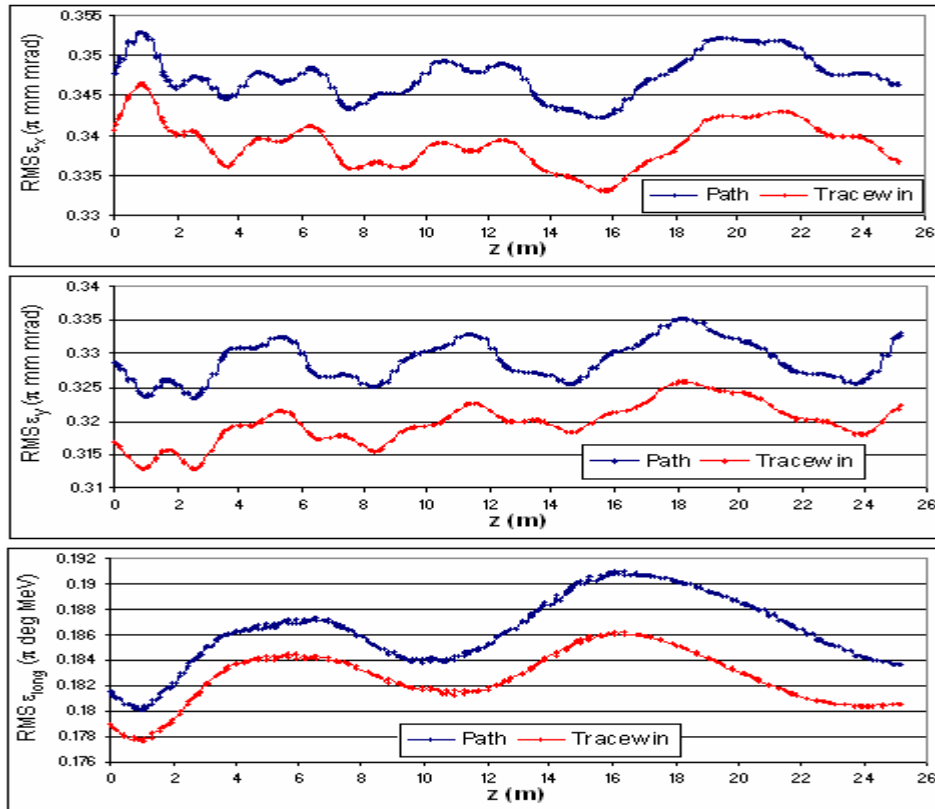


Figure 52: RMS emittances along the CCDTL, beam from the DTL, $I = 62$ mA

Table 42: Maximum difference between the RMS beam size, beam from the DTL, I = 62 mA

Max $\Delta x_{RMS}/x_{RMS}$	Max $\Delta y_{RMS}/y_{RMS}$	Max $\Delta \text{phase}_{RMS}/\text{phase}_{RMS}$
4.6%	6.4%	-2.0%

Table 43: Maximum difference between the emittances, beam from the DTL, I = 62 mA

Max $\Delta \epsilon_x/\epsilon_x$	Max $\Delta \epsilon_y/\epsilon_y$	Max $\Delta \epsilon_{long}/\epsilon_{long}$
2.8%	3.2%	3%

The RMS and 90% emittance growth in the CCDTL are reported in Tables 44 and 45.

Table 44: RMS emittance growth in the CCDTL

	ϵ_x	ϵ_y	ϵ_{long}
PATH	-0.4%	1.4%	1.1%
TRACEWIN	-1.1%	1.7%	0.8%

Table 45: 90% emittance growth in the CCDTL

	ϵ_x	ϵ_y	ϵ_{long}
PATH	-2.4%	1.2%	-1.1%
TRACEWIN	-0.6%	3.0%	-0.6%

3.5 Summary for the CCDTL

The check with a generated beam shows that the structure is treated the same way both in PATH and TRACEWIN. In fact, without space charge effects, the RMS beam sizes are practically the same, the RMS emittances are very similar with a maximum $\Delta\epsilon/\epsilon$ of 0.15% (ϵ_{long}) and we have equal transmissions.

Considering space charge effects, the results are still very good, with a maximum $\Delta\epsilon/\epsilon$ of 0.9% (ϵ_{long}) and the difference between the RMS beam size envelopes is under 3%.

Using the beam coming from the DTL, the differences become greater, especially without space charge effects: the difference in RMS emittance is between 1.4% and 7.7% and the difference in RMS beam size is 15% to 22% (in absolute value).

With space charge, these differences are about 3% for emittances and between 2% and 6.5% for RMS beam size. Moreover, the beam RMS characteristics are very similar.

All these differences between the output beams are probably due to the differences in the input beam, caused by the different ways PATH and TRACEWIN treat the DTL cell. This effect is partially overridden by the space-charge.

4. Beam dynamics in the SCL

The SCL operates at twice the frequency of the preceding structures. As the beam current used in the simulations is defined per RF frequency, the beam current in the SCL simulations has to be doubled with respect to the beam current used in the preceding structures. The longitudinal beam parameters related to the RF frequency have to be doubled as well.

The output energy is 180 MeV (24 tanks, 34.433 m) when the Linac4 injects in the SPL, and 160 MeV (20 tanks, 28.046 m), to inject into the PS Booster. The simulations have been performed until 180 MeV

In order to check the structure of the SCL in both codes, the first runs have been done with a generated input beam. Once the structure is checked the runs have been performed with the beam coming from the CCDTL, with and without space charge.

4.1 Test beam, $I = 0$ mA

The characteristics of the generated input beam are:

- Number of particles = 50000
- $f = 704.4$ MHz
- $E_{in} = 90$ MeV
- Twiss parameters:

	α	β	$\epsilon_{RMS,N}$
x	3.91	6.03 mm/ π mrad	0.30 π mm mrad
y	-1.10	1.56 mm/ π mrad	0.30 π mm mrad
long	0.11	44.67 deg/ π MeV	0.37 π deg MeV

Without space charge effects, the transmission in the SCL is 100% in both codes. The energy evolution is plotted in Figure 53. The final energy is 180.18 MeV in PATH and 180.23 MeV in TRACEWIN, respectively.

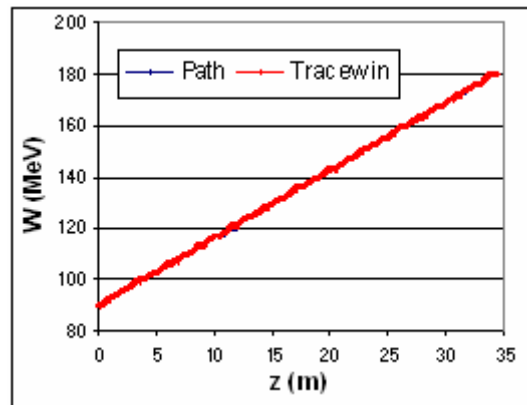


Figure 53: Energy evolution along the SCL, test beam, $I = 0$ mA

The SCL output beam shapes are presented in Figures 54 and 55. Twiss parameters are reported in Tables 46 and 47, obtained respectively with TRACEWIN and PATH.

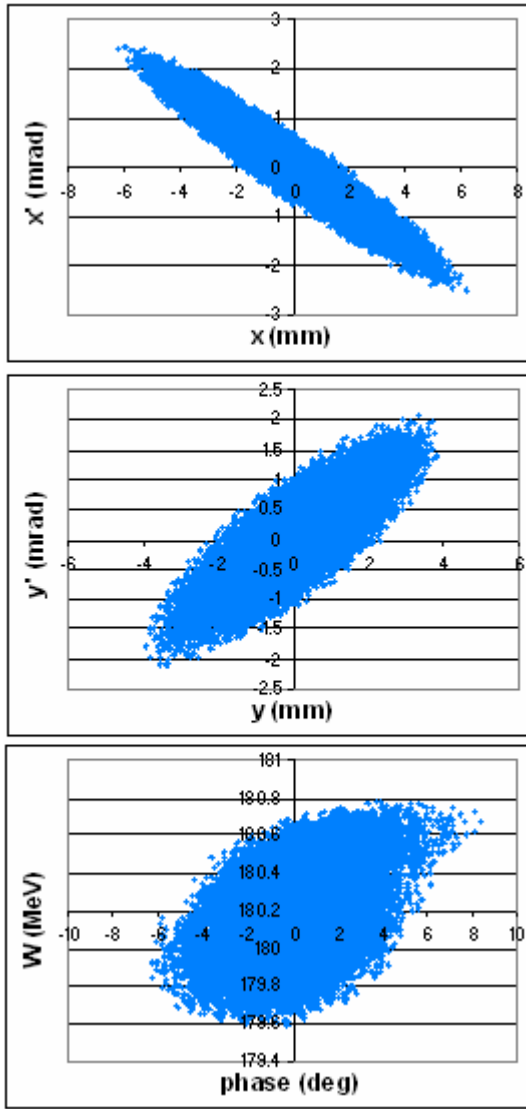


Figure 54: SCL output beam in PATH, test beam, $I = 0$ mA

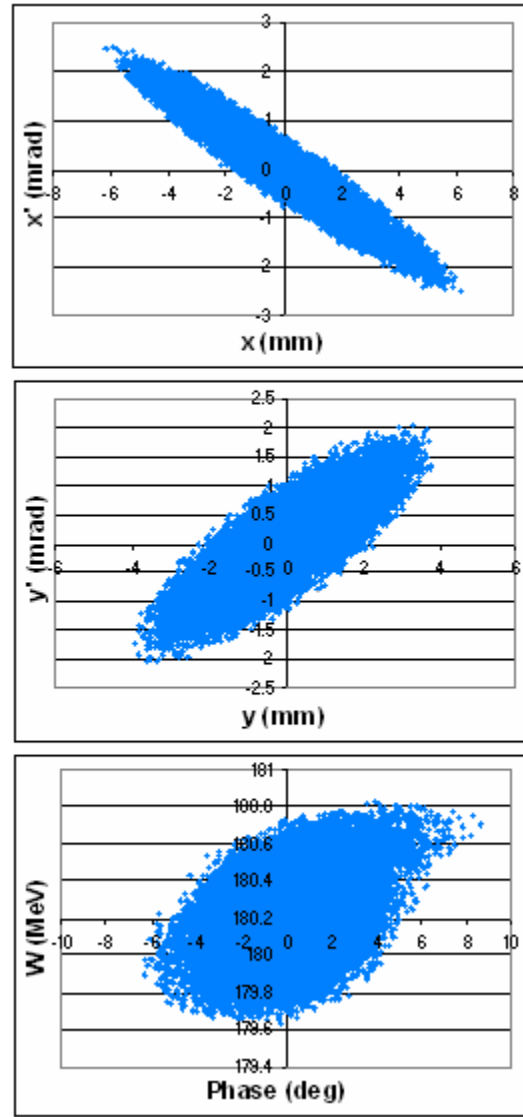


Figure 55: SCL output beam in TRACEWIN, test beam, $I = 0$ mA

Table 46: SCL output beam Twiss parameters in TRACEWIN, test beam, $I = 0$ mA

	α	β	$\epsilon_{RMS,N}$	$\epsilon_{90\%,N}$
x	3.16	8.09 mm/ π mrad	0.30 π mm mrad	1.37 π mm mrad
y	-1.36	3.32 mm/ π mrad	0.30 π mm mrad	1.37 π mm mrad
long	-0.49	10.50 deg/ π MeV	0.38 π deg MeV	1.69 π deg MeV

Table 47: SCL output beam Twiss parameters in PATH, test beam, $I = 0$ mA

	α	β	$\epsilon_{RMS,N}$	$\epsilon_{90\%,N}$
x	3.16	8.10 mm/ π mrad	0.30 π mm mrad	1.36 π mm mrad
y	-1.38	3.32 mm/ π mrad	0.30 π mm mrad	1.36 π mm mrad
long	-0.47	10.22 deg/ π MeV	0.38 π deg MeV	1.68 π deg MeV

The RMS beam size envelopes and emittances are plotted in Figures 56 and 57.

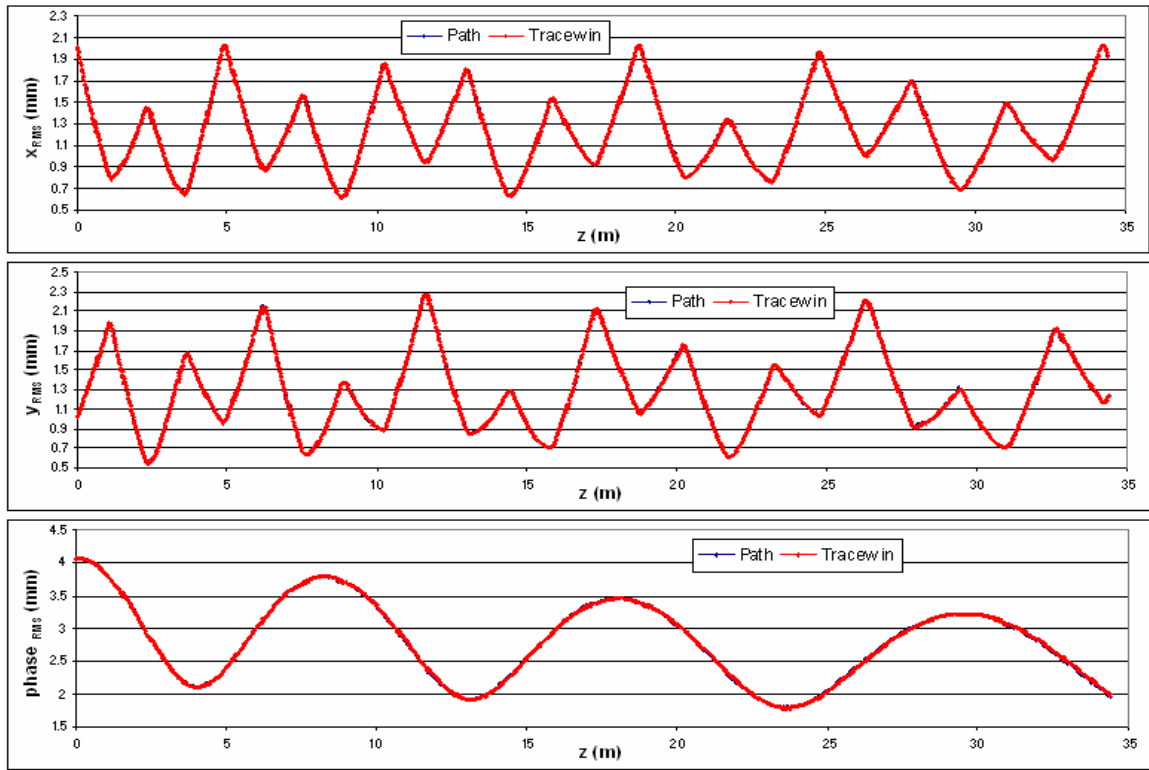


Figure 56: RMS beam size envelopes along the SCL, test beam, $I = 0$ mA

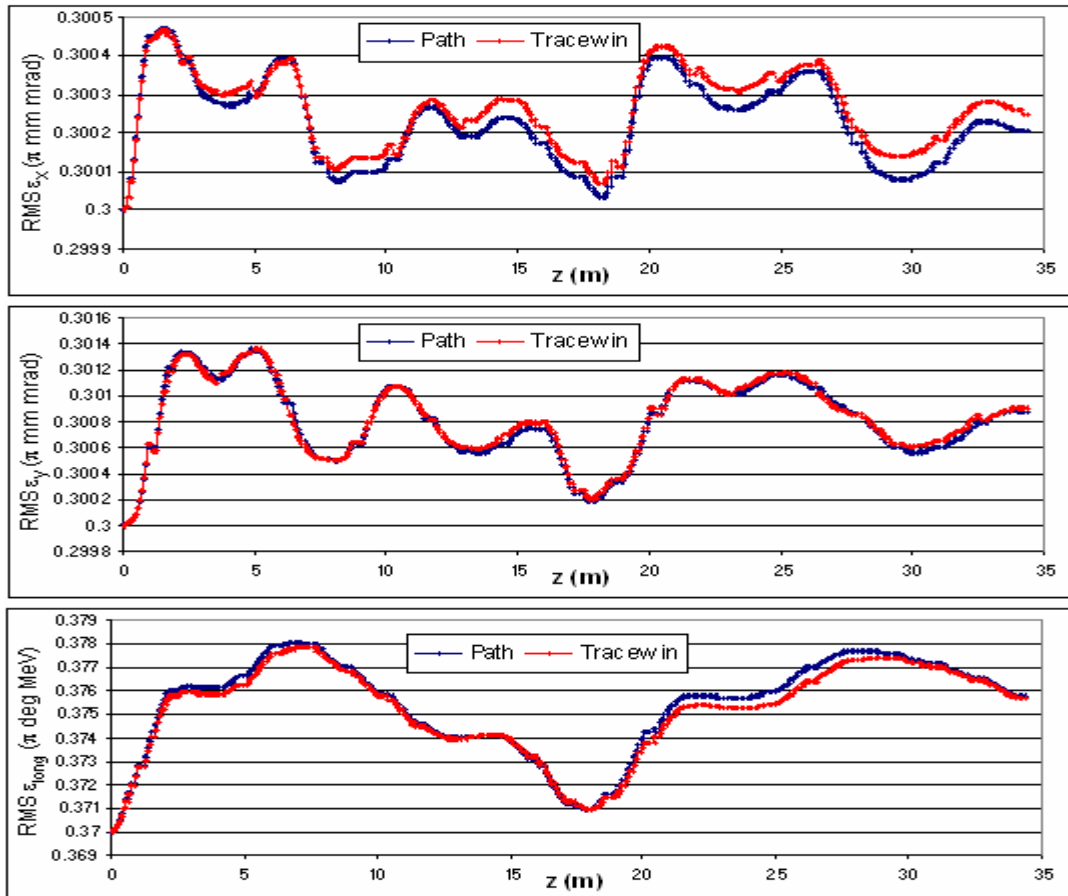


Figure 57: RMS normalized emittance evolution along the SCL, test beam, $I = 0$ mA

The maximum difference between the emittances is reported in Table 48, taking the TRACEWIN results as reference $((X_{\text{PATH}} - X_{\text{TRACEWIN}}) / X_{\text{TRACEWIN}})$.

Table 48: Maximum difference between the emittances, test beam, I = 0 mA

Max $\Delta\varepsilon_x/\varepsilon_x$	Max $\Delta\varepsilon_y/\varepsilon_y$	Max $\Delta\varepsilon_{\text{long}}/\varepsilon_{\text{long}}$
-0.02%	-0.03%	-0.13%

4.2 Test beam, I = 130 mA

The transmission is 100% in both codes. The energy evolution along the SCL is plotted in Figure 57. The final energy is 180.24 MeV in TRACEWIN and 180.15 MeV in PATH.

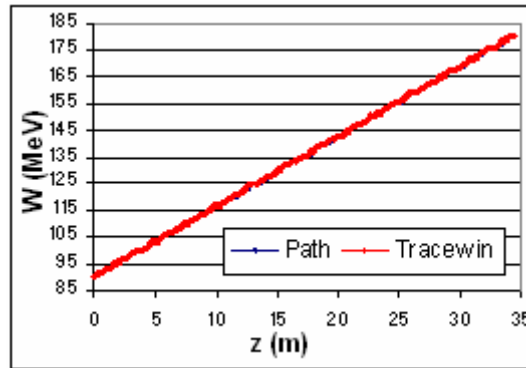


Figure 58: Energy evolution along the SCL, test beam, I = 130 mA

The SCL output beam shapes are plotted In Figures 59 and 60. Twiss parameters are reported in Tables 49 and 50, obtained respectively with TRACEWIN and PATH.

Table 49: SCL output beam Twiss parameters in TRACEWIN, test beam, I = 130 mA

	α	β	$\varepsilon_{\text{RMS},N}$	$\varepsilon_{90\%,N}$
x	2.98	7.66 mm/ π mrad	0.31 π mm mrad	1.42 π mm mrad
y	-1.11	3.07 mm/ π mrad	0.32 π mm mrad	1.44 π mm mrad
long	0.04	24.60 deg/ π MeV	0.38 π deg MeV	1.69 π deg MeV

Table 50: SCL output beam Twiss parameters in PATH, test beam, I = 130 mA

	α	β	$\varepsilon_{\text{RMS},N}$	$\varepsilon_{90\%,N}$
x	3.14	8.18 mm/ π mrad	0.31 π mm mrad	1.42 π mm mrad
y	-1.25	3.28 mm/ π mrad	0.32 π mm mrad	1.45 π mm mrad
long	0.03	26.24 deg/ π MeV	0.39 π deg MeV	1.68 π deg MeV

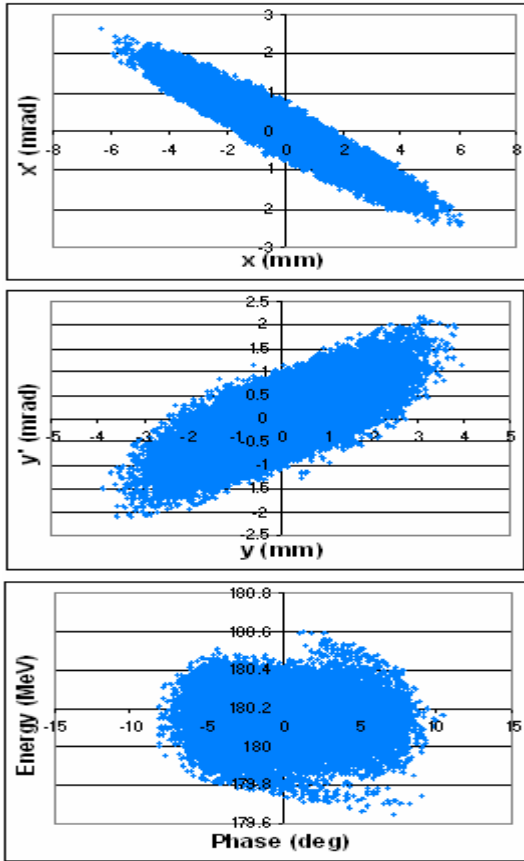


Figure 59: SCL output beam in PATH, test beam, $I = 130$ mA

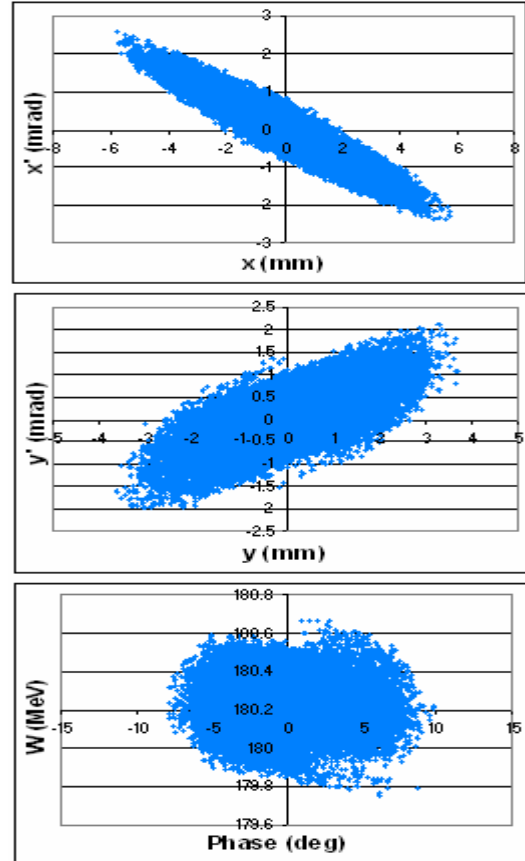


Figure 60: SCL output beam in TRACEWIN, test beam, $I = 130$ mA

The RMS beam size envelopes and emittances are plotted in Figures 61 and 62.

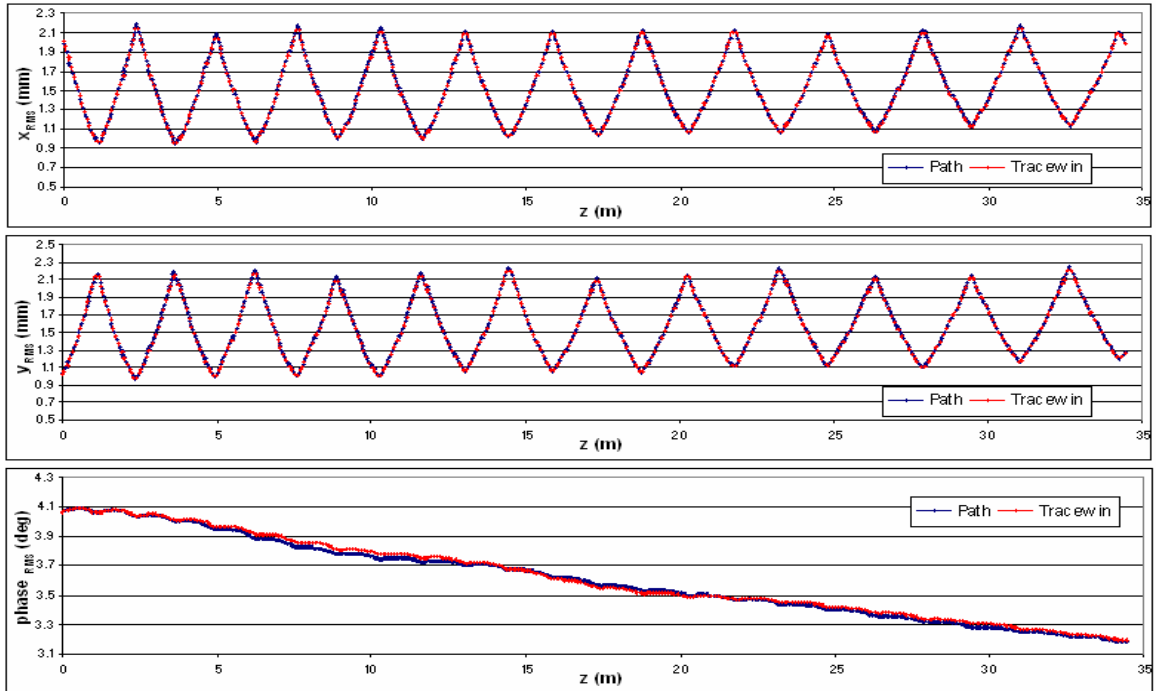


Figure 61: RMS beam size envelopes along the SCL, test beam, $I = 130$ mA

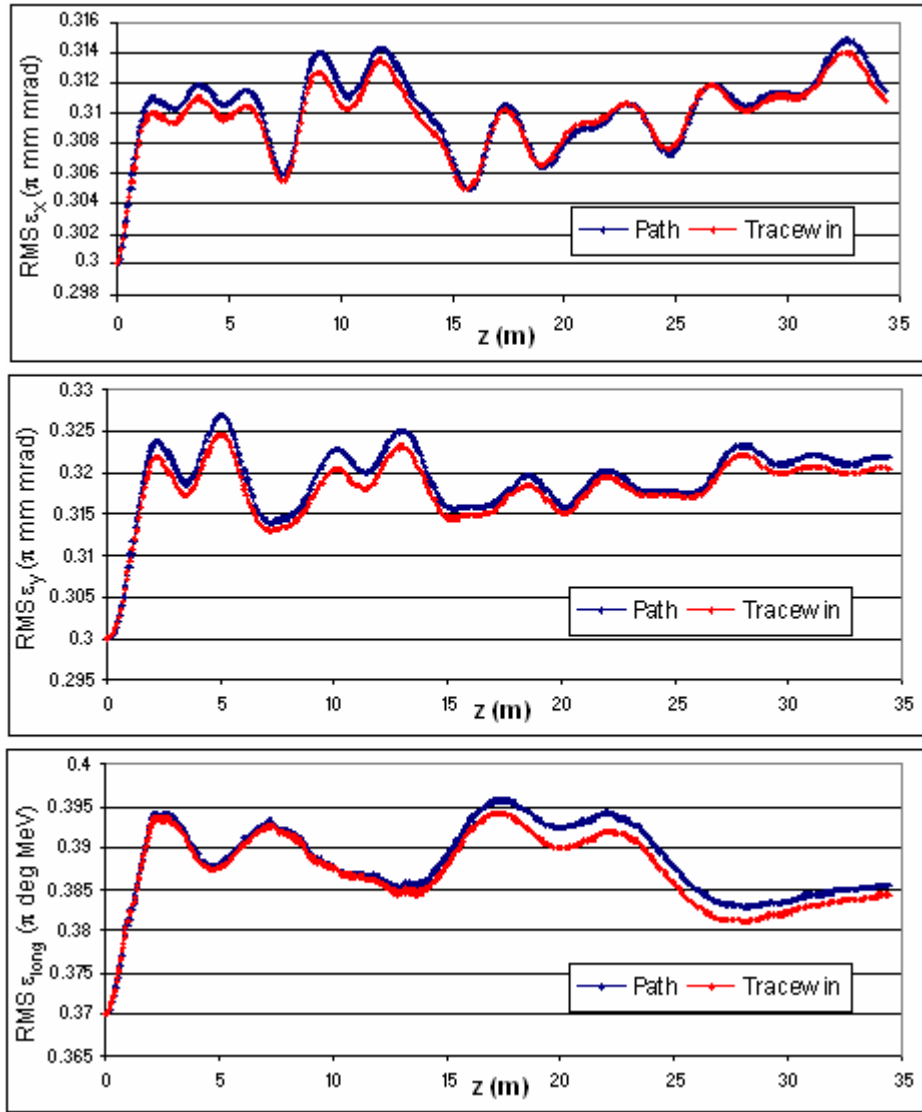


Figure 62: RMS normalized emittance evolution along the SCL, test beam, $I = 130$ mA

As for the runs with no space-charge effects, there is no significant difference between the RMS transverse sizes. And for the RMS phases the maximum difference is just 0.8%.

Table 51: Maximum difference between the emittances, test beam, $I = 130$ mA

$\text{Max } \Delta\epsilon_x/\epsilon_x$	$\text{Max } \Delta\epsilon_y/\epsilon_y$	$\text{Max } \Delta\epsilon_{\text{long}}/\epsilon_{\text{long}}$
0.4%	0.7%	0.6%

4.3 Beam from the CCDTL, unmatched case ($I = 0$ mA)

The output energy of the SCL is 180 MeV in case of the SPL and 160 MeV in case of Linac4. For both output energies the transmission is 99.57% in TRACEWIN and 99.59% in PATH. The beam losses along the SCL are plotted in Figure 63.

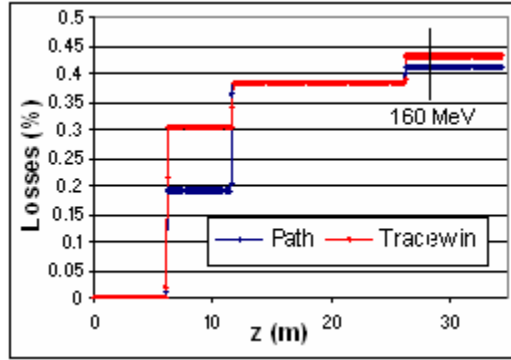


Figure 63: Beam losses along the SCL, beam from the CCDTL, unmatched case

At the output of the 20th tank the beam energy is 163.61 MeV in PATH and 163.13 MeV in TRACEWIN. At the output of the 24th tank the beam energy is 180.42 MeV in PATH and 179.86 MeV in TRACEWIN.

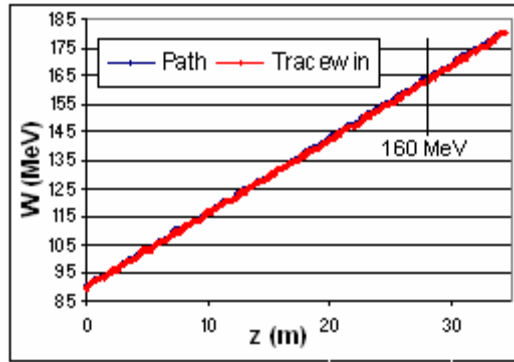


Figure 64: Energy evolution along the SCL, beam from the CCDTL, unmatched case

Figures 65-68 present the SCL output beam shapes for both energies. Twiss parameters are reported in Tables 52-55.

Table 52: SCL output beam Twiss parameters in TRACEWIN @ 160 MeV, beam from the CCDTL, unmatched case

	α	β	$\epsilon_{RMS,N}$	$\epsilon_{90\%,N}$
x	3.57	5.53 mm/ π mrad	0.39 π mm mrad	1.68 π mm mrad
y	0.22	6.83 mm/ π mrad	0.89 π mm mrad	4.29 π mm mrad
long	0.48	15.27 deg/ π MeV	0.40 π deg MeV	1.88 π deg MeV

Table 53: SCL output beam Twiss parameters in PATH @ 160 MeV, beam from the CCDTL, unmatched case

	α	β	$\epsilon_{RMS,N}$	$\epsilon_{90\%,N}$
x	2.54	3.80 mm/ π mrad	0.39 π mm mrad	1.68 π mm mrad
y	0.29	5.92 mm/ π mrad	1.00 π mm mrad	4.75 π mm mrad
long	0.41	12.73 deg/ π MeV	0.44 π deg MeV	2.07 π deg MeV

Table 54: SCL output beam Twiss parameters in TRACEWIN @ 180 MeV, beam from the CCDTL, unmatched case

	α	β	$\epsilon_{RMS,N}$	$\epsilon_{90\%,N}$
x	6.71	15.94 mm/ π mrad	0.38 π mm mrad	1.65 π mm mrad
y	-6.56	12.87 mm/ π mrad	0.85 π mm mrad	3.96 π mm mrad
long	-0.52	15.91 deg/ π MeV	0.37 π deg MeV	1.72 π deg MeV

Table 55: SCL output beam Twiss parameters in PATH @ 180 MeV, beam from the CCDTL, unmatched case

	α	β	$\epsilon_{RMS,N}$	$\epsilon_{90\%,N}$
x	6.12	13.74 mm/ π mrad	0.39 π mm mrad	1.69 π mm mrad
y	-5.62	11.28 mm/ π mrad	0.98 π mm mrad	4.48 π mm mrad
long	-0.40	19.89 deg/ π MeV	0.41 π deg MeV	1.94 π deg MeV

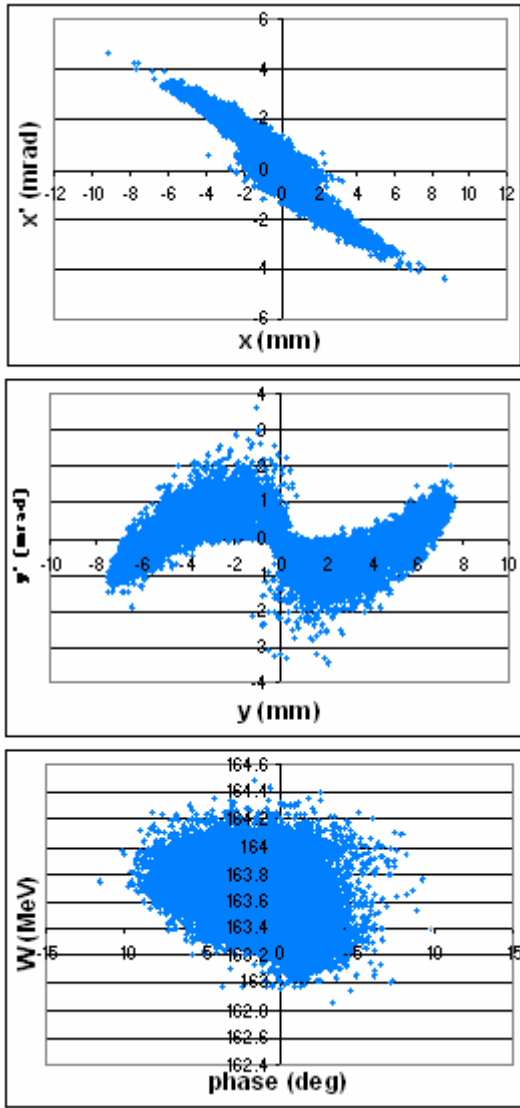


Fig. 65: CCDTL output beam in PATH @ 160 MeV, beam from the CCDTL, unmatched case

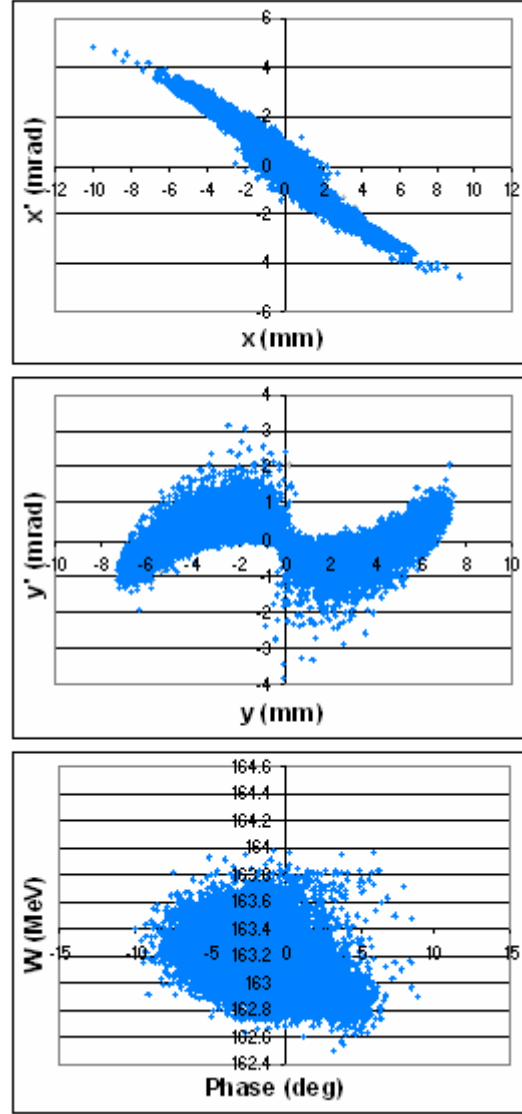


Fig. 66: SCL output beam in TRACEWIN @ 160 MeV, beam from the CCDTL, unmatched case

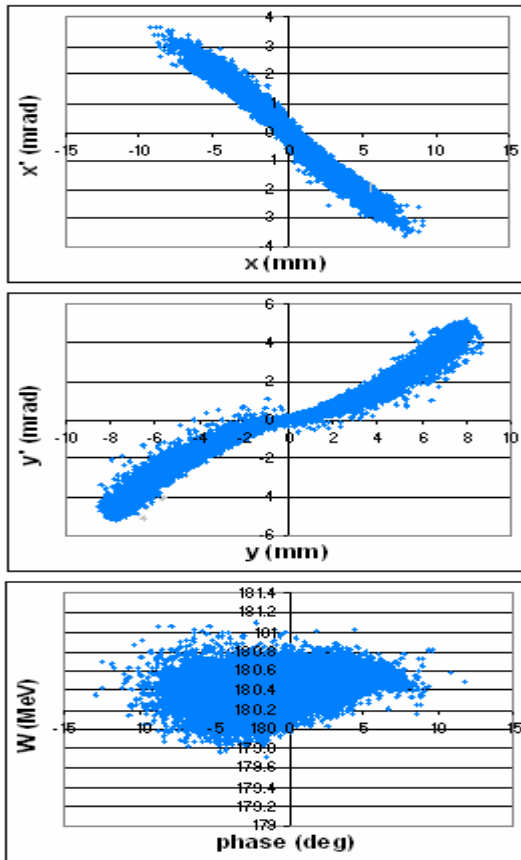


Fig. 67: CCDTL output beam in PATH @ 180 MeV, beam from the CCDTL, unmatched case

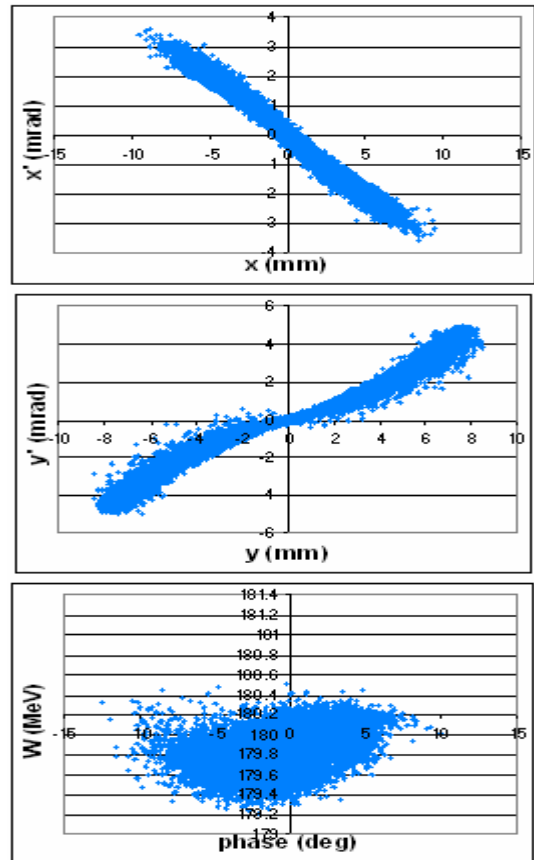


Fig. 68: SCL output beam in TRACEWIN @ 180 MeV, beam from the CCDTL, unmatched case

The RMS beam size envelopes and emittances are plotted in Figures 69 and 70.

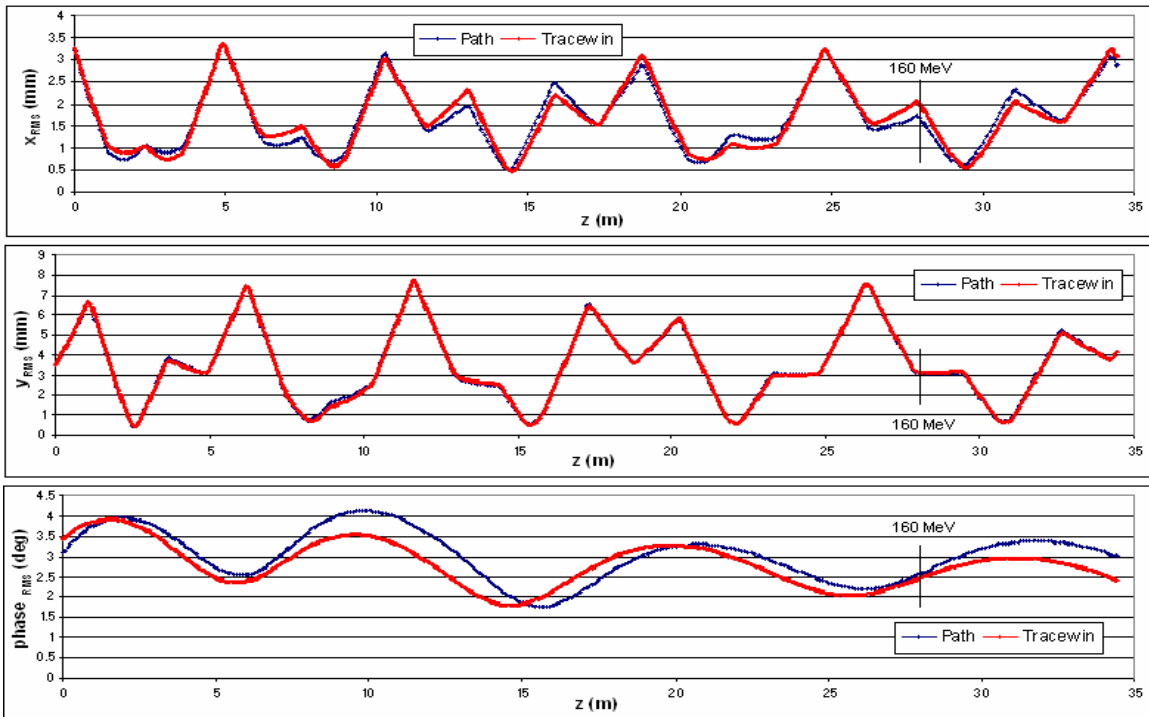


Figure 69: RMS beam size envelopes along the SCL, beam from the CCDTL, unmatched case

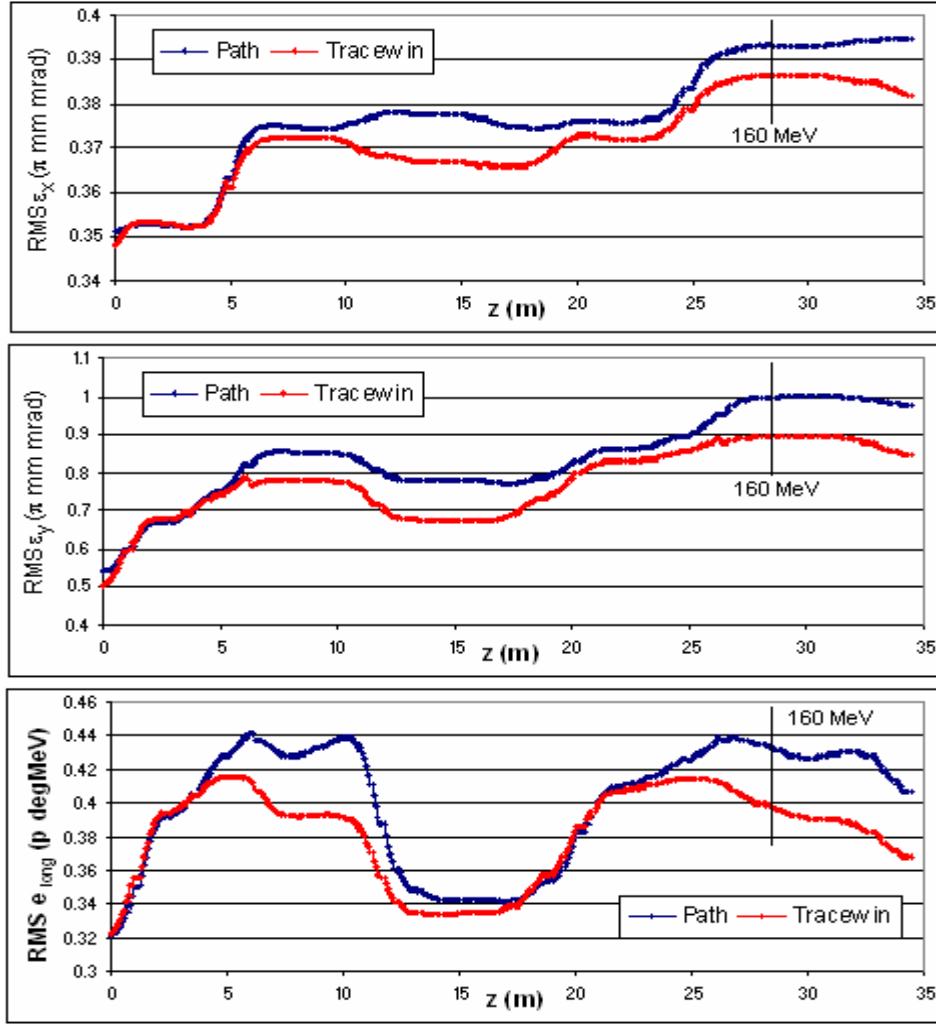


Figure 70: RMS emittances evolution along the SCL, beam from the CCDTL, unmatched case

The maximum difference between the values in above plotted graphs is presented in Tables 56 and 57.

Table 56: Maximum difference between the RMS sizes, beam from the CCDTL, unmatched case

Max $\Delta x_{RMS}/x_{RMS}$	Max $\Delta y_{RMS}/y_{RMS}$	Max $\Delta \text{phase}_{RMS}/\text{phase}_{RMS}$
-15.6%	17.3%	20.8%

Table 57: Maximum difference between the emittances, beam from the CCDTL, unmatched case

Max $\Delta \epsilon_x/\epsilon_x$	Max $\Delta \epsilon_y/\epsilon_y$	Max $\Delta \epsilon_{long}/\epsilon_{long}$
3.4%	15.4%	12.3%

4.4 Beam from the CCDTL, matched case

The beam current is 124.4 mA in TRACEWIN and 123.8 mA in PATH, doubled with respect to the current in the previous structures to account for the frequency change. The difference in values is mainly due to the difference in the transmission in the Chopper Line.

The transmission in the SCL is 100% in both codes. The final energy at the output of the 20th tank is 163.05 MeV in PATH and 163.13 MeV in TRACEWIN and at the output of the 24th tank the energy is 179.83 MeV in PATH and 179.89 MeV in TRACEWIN, so the difference between the values in the two codes $\Delta W/W$ is under 0.05% (in absolute value).

The SCL output beam shapes at both energies are represented in Figures 71-74. Twiss parameters are reported in Tables 58-61.

Table 58: SCL output beam Twiss parameters in TRACEWIN @ 160 MeV, beam from CCDTL, I = 124 mA

	α	β	$\epsilon_{RMS,N}$	$\epsilon_{90\%,N}$
x	3.07	7.57 mm/ π mrad	0.34 π mm mrad	1.46 π mm mrad
y	-1.15	2.62 mm/ π mrad	0.33 π mm mrad	1.46 π mm mrad
long	0.05	28.70 deg/ π MeV	0.37 π deg MeV	1.73 π deg MeV

Table 59: SCL output beam Twiss parameters in PATH @ 160 MeV, beam from CCDTL, I = 124 mA

	α	β	$\epsilon_{RMS,N}$	$\epsilon_{90\%,N}$
x	3.08	7.56 mm/ π mrad	0.35 π mm mrad	1.42 π mm mrad
y	-1.11	2.61 mm/ π mrad	0.35 π mm mrad	1.49 π mm mrad
long	0.04	28.40 deg/ π MeV	0.38 π deg MeV	1.72 π deg MeV

Table 60: SCL output beam Twiss parameters in TRACEWIN @ 180 MeV, beam from CCDTL, I = 124 mA

	α	β	$\epsilon_{RMS,N}$	$\epsilon_{90\%,N}$
x	3.05	7.88 mm/ π mrad	0.35 π mm mrad	1.49 π mm mrad
y	-1.14	2.95 mm/ π mrad	0.33 π mm mrad	1.43 π mm mrad
long	0.01	25.85 deg/ π MeV	0.37 π deg MeV	1.74 π deg MeV

Table 61: SCL output beam Twiss parameters in PATH @ 180 MeV, beam from CCDTL, I = 124 mA

	α	β	$\epsilon_{RMS,N}$	$\epsilon_{90\%,N}$
x	3.00	7.79 mm/ π mrad	0.35 π mm mrad	1.48 π mm mrad
y	-1.14	2.93 mm/ π mrad	0.35 π mm mrad	1.42 π mm mrad
long	0.01	25.59 deg/ π MeV	0.38 π deg MeV	1.71 π deg MeV

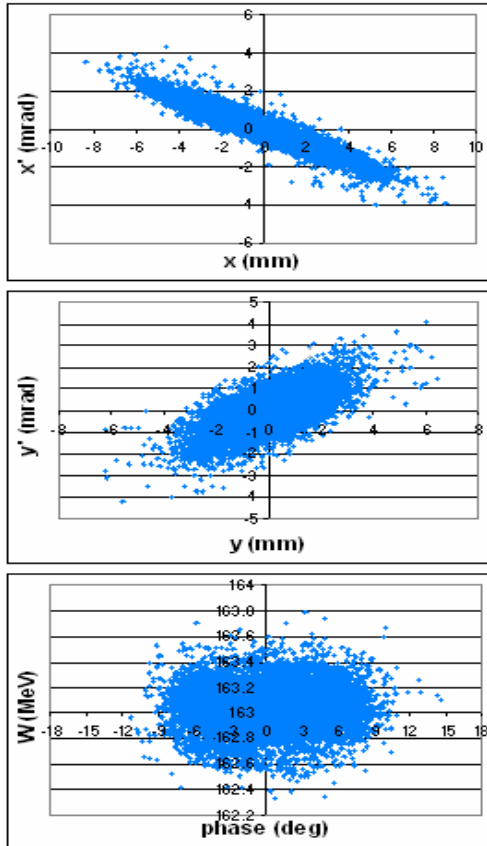


Fig. 71: SCL output beam in PATH @ 160 MeV, beam from the CCDTL, I = 124 mA

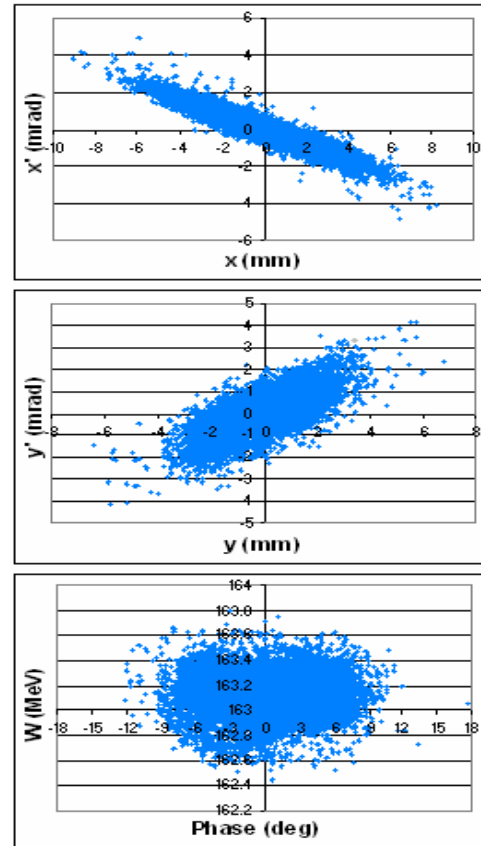


Fig. 72: SCL output beam in TRACEWIN @ 160 MeV, beam from the CCDTL, I = 124 mA

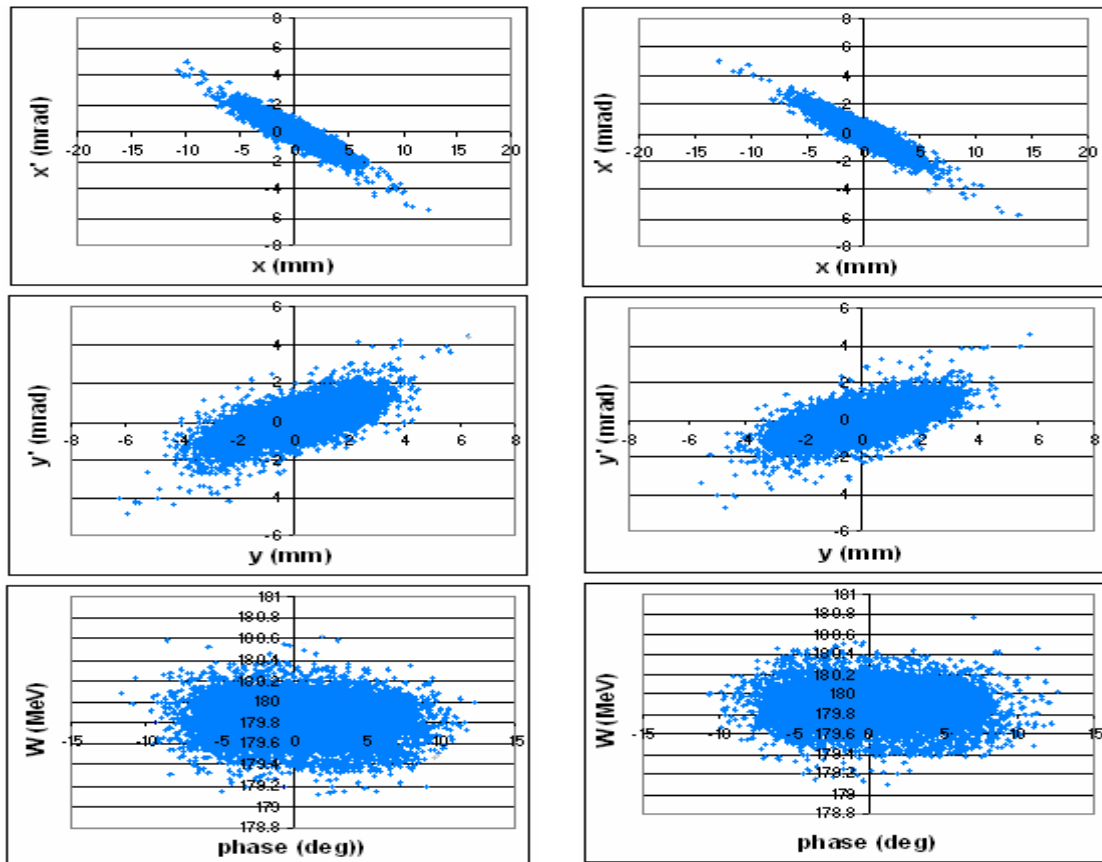


Fig. 73: SCL output beam in PATH @ 180 MeV, Fig. 74: SCL output beam in TRACEWIN @ 180 MeV, beam from the CCDTL, $I = 124$ mA

The RMS beam size envelopes and emittances are plotted in Figures 75 and 76.

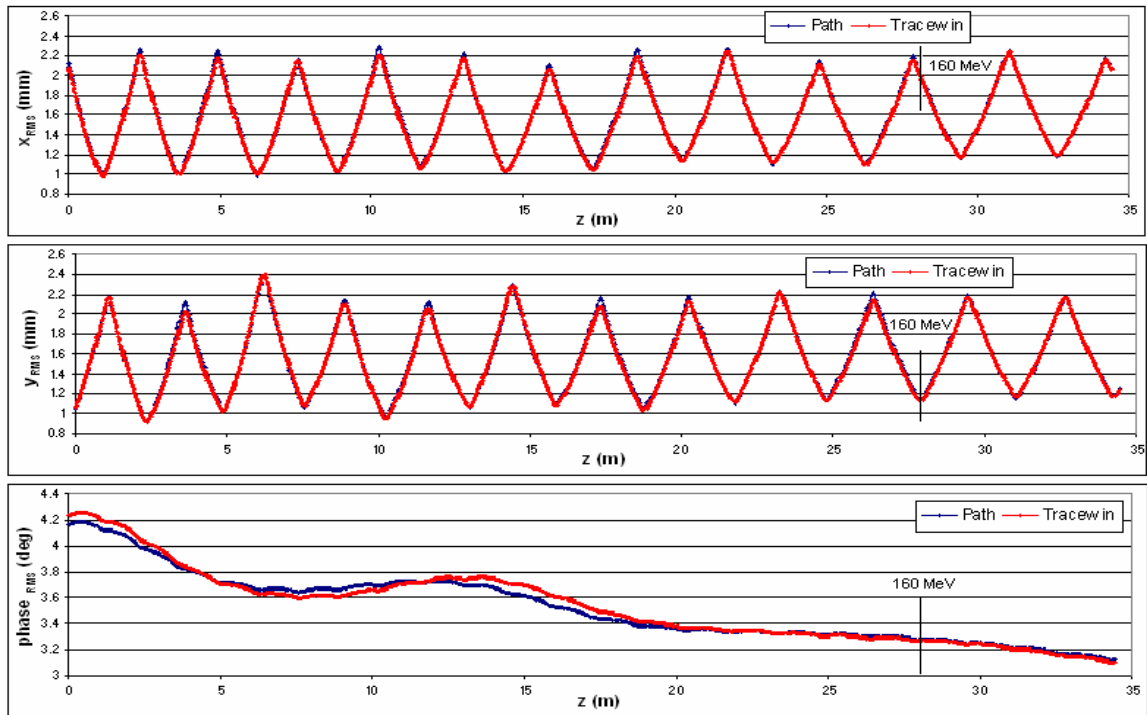


Figure 75: RMS beam size envelopes along the SCL, beam from the CCDTL, $I = 124$ mA

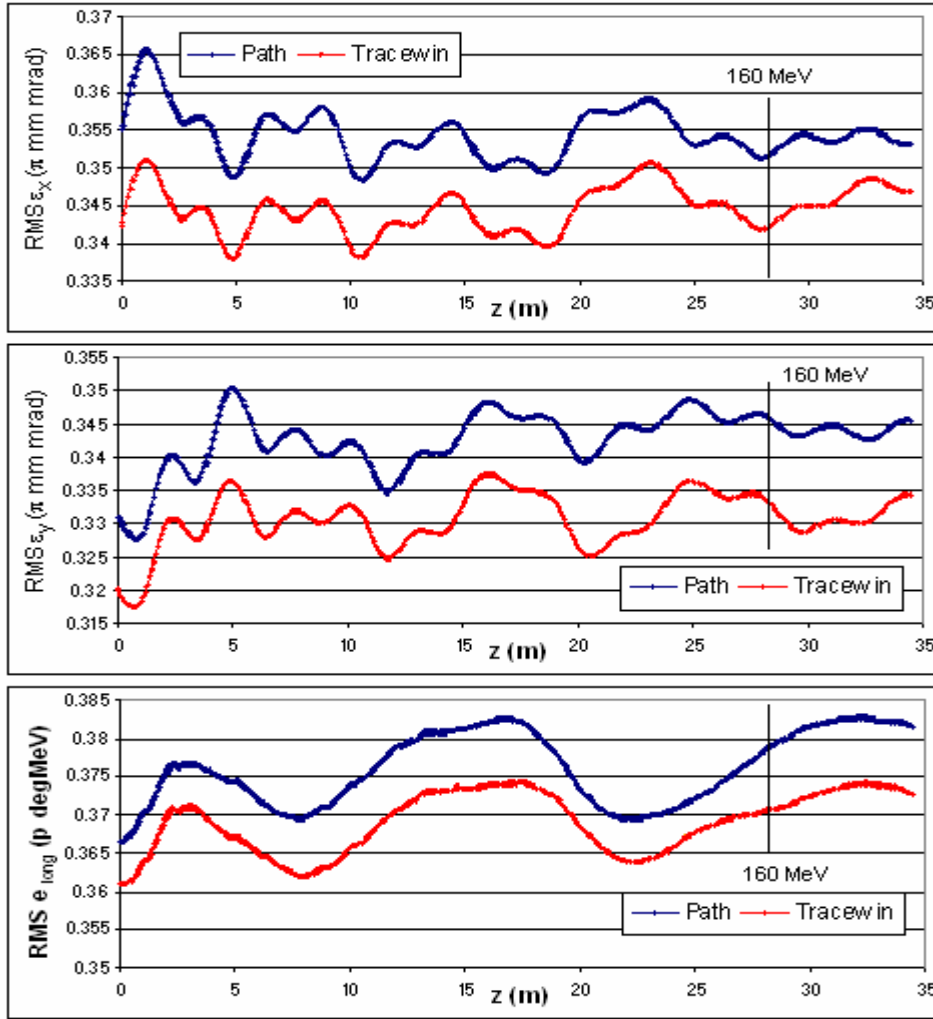


Figure 76: RMS emittances along the SCL, beam from the CCDTL, I = 124 mA

Table 62: Maximum difference between the RMS beam size envelopes, beam from the CCDTL, I = 124 mA

Max $\Delta x_{RMS}/x_{RMS}$	Max $\Delta y_{RMS}/y_{RMS}$	Max $\Delta \text{phase}_{RMS}/\text{phase}_{RMS}$
3.4%	5.1%	-2.2%

Table 63: Maximum difference between the emittances, beam from the CCDTL, I = 124 mA

Max $\Delta \epsilon_x/\epsilon_x$	Max $\Delta \epsilon_y/\epsilon_y$	Max $\Delta \epsilon_{long}/\epsilon_{long}$
4%	4.6%	2.2% (2.4% after 160MeV)

The RMS and 90% emittance growth in the SCL is reported in Tables 64-67.

Table 64: RMS emittance growth in the SCL @ 160 MeV

	ϵ_x	ϵ_y	ϵ_{long}
PATH	-1.0%	4.6%	3.3%
TRACEWIN	-0.1%	4.3%	2.7%

Table 65: 90% emittance growth in the SCL @ 160 MeV

	ϵ_x	ϵ_y	ϵ_{long}
PATH	-3.2%	9.1%	1.5%
TRACEWIN	-0.05%	6.1%	1.4%

Table 66: RMS emittance growth in the SCL @ 180 MeV

	ϵ_x	ϵ_y	ϵ_{long}
PATH	-0.5%	4.3%	4.1%
TRACEWIN	1.3%	4.4%	3.2%

Table 67: 90% emittance growth in the SCL @ 180 MeV

	ϵ_x	ϵ_y	ϵ_{long}
PATH	0.4%	3.8%	0.9%
TRACEWIN	2.0%	4.3%	2.4%

4.5 Summary for the SCL

The check with the generated beam shows that the structure is treated in the same way both in PATH and in TRACEWIN. In fact, without space charge effects, the RMS beam sizes are practically the same. The RMS emittances are very similar with maximum difference of $\Delta\epsilon/\epsilon = 0.13\%$ (ϵ_{long}) and the transmission is the same in both codes.

With space charge, the results are still very good, with maximum difference of $\Delta\epsilon/\epsilon = 0.7\%$ (ϵ_{long}) and the difference between the RMS beam sizes is less than 1%.

Using the beam coming from the output of the previous structure, the differences become greater and the case without space-charge effect is the worst. In case of simulations with no space-charge the difference between the RMS emittances is between 3% and 16% and the difference between the RMS beam sizes is between 16% and 21% (in absolute value). In the simulations with space-charge the RMS emittances differ by about 4%, except for the longitudinal (about 2%). The difference in the values of the RMS beam sizes is between 2% and 5%.

All these differences between the output beams are probably due to the differences in the input beams, caused by the different ways PATH and TRACEWIN treat the DTL cell and it is partially overridden by the space-charge.

Conclusion and outlook

Linac4 has been simulated from 3 to 180 MeV with the codes Path and Tracewin: the results agree to better than 10% everywhere.

End-to-end simulation has shown that the beam losses are practically all in the Chopper Line dump (11% for the matched case, 36% for the fully unmatched case). The major emittance growth is in the Chopper Line and, in the case of the vertical emittance, in the DTL, so the structures are well matched.

The simulations presented in this note start at the beginning of the RFQ; in future the simulations should include the LEPT and the transfer line to the PS Booster in order to perform a complete end-to-end simulation, from the source output to the Booster injection.

Reference

- [1] CONCEPTUAL DESIGN OF THE SPL II, A High Power Superconducting H- Linac at CERN, 2006
- [2] P.-Y. Beauvais, "Recent evolutions in the design of the French high intensity proton injector (IPHI)", Proc. European Particle Accelerator Conf., Lucerne, Switzerland, 2004.
- [3] A. Perrin, J.-F. Amand, T. Muetze, "Travel User Manual"
- [4] R. Duperrier, N. Pichoff, D. Uriot, "CEA Saclay codes review", ICCS Conference 2002, Amsterdam
- [5] R. Duperrier, "Toutatis, a radio-frequency quadrupole code", Phys. Rev, Spec. Top. Acc. & Beams, December 2000.